

MOL #33035

**The α_{1b} -adrenoceptor exists as a higher-order oligomer: effective oligomerization
is required for receptor maturation, surface delivery and function**

Juan F. Lopez-Gimenez, Meritxell Canals, John D. Padiani and Graeme Milligan

Molecular Pharmacology Group, Division of Biochemistry and Molecular Biology
Institute of Biomedical and Life Sciences, University of Glasgow, Glasgow G12 8QQ
Scotland, U.K.

MOL #33035

Running title: Oligomerization of the α_{1b} -adrenoceptor

Correspondence to:

Graeme Milligan, Davidson Building, University of Glasgow, Glasgow, Scotland,

U.K.

Tel 44 141 330 5557, FAX 44 141 330 4620, e-mail: g.milligan@bio.gla.ac.uk

number of text pages: 51

number of Tables: 0

number of Figures: 13

number of references: 37

number of words in Abstract: 250

number of words in Introduction: 623

number of words in Discussion: 1500

Abbreviations: FRET, fluorescence resonance energy transfer; GPCR, G protein-coupled receptor; TMD, transmembrane domain; QAPB, BODIPY-FL prazosin; RQAPB, red BODIPY-FL prazosin

MOL #33035

ABSTRACT

Approaches to identify G protein-coupled receptor oligomers rather than dimers have been lacking. Using concatamers of fluorescent proteins we established conditions to monitor sequential three color fluorescence resonance energy transfer (3-FRET) and used these to detect oligomeric complexes of the α_{1b} -adrenoceptor in single living cells. Mutation of putative key hydrophobic residues in transmembrane domains I and IV resulted in substantial reduction of sequential 3-FRET and was associated with lack of protein maturation, prevention of plasma membrane delivery and elimination of signalling function. Although these mutations prevented cell surface delivery, bi-molecular fluorescence complementation studies indicated they did not ablate protein-protein interactions and confirmed endoplasmic reticulum/Golgi retention of the transmembrane domain I + transmembrane domain IV mutated receptor. The transmembrane domain I + transmembrane domain IV mutated receptor was a 'dominant negative' in blocking cell surface delivery of the wild type receptor. Mutations only in transmembrane domain I did not result in a reduction in 3-FRET, whilst restricting mutation to transmembrane domain IV did result in reduced 3-FRET. Mutations in either transmembrane domain I or transmembrane domain IV were, however, sufficient to eliminate cell surface delivery. Terminal N-glycosylation is insufficient to determine cell surface delivery because both the transmembrane domain I and transmembrane domain IV mutants matured as effectively as the wild type receptor. These data indicate that the α_{1b} -adrenoceptor is able to form oligomeric, rather than only simple dimeric complexes, and that disruption of

MOL #33035

effective oligomerization by introducing mutations into transmembrane domain IV
has profound consequences for cell surface delivery and function.

MOL #33035

In recent times it has become widely accepted that many (Milligan, 2004; Park et al., 2004) but perhaps not all (Meyer et al., 2006) members of the rhodopsin-like, family A, G protein-coupled receptor (GPCR) group possess quaternary structure. It has been suggested that these receptors exist, and probably function, as dimers (Baneres and Parello, 2003; Fotiadis et al., 2004). Recently, the application of atomic force microscopy to membranes of murine rod outer segments demonstrated complex *in situ* quaternary organization of rhodopsin in that paracrystalline rows or oligomers of dimers were observed (Liang et al., 2003). This allowed interaction interfaces to be predicted and modelled (Fotiadis et al., 2004). The rod outer segment is, however, a highly specialized structure in which rhodopsin comprises close to 50% of the total protein. By contrast, many GPCRs in other tissues are expressed in relatively low amounts. It is therefore unclear if the *in situ* oligomeric organization of rhodopsin is relevant to other GPCRs or to other environments. Recently, however, molecules of rhodopsin reconstituted into asolectin liposomes were shown to self-associate into dimers or multimers (Mansoor et al., 2006) and this has been suggested to provide evidence that rhodopsin can spontaneously self-associate in membranes other than the rod outer segment (Mansoor et al., 2006). Although approaches used to examine interactions between GPCR monomers have developed from initial co-immunoprecipitation studies to the application of a range of resonance energy transfer-based techniques (Milligan and Bouvier, 2005), these are generally unable to determine whether quaternary structure is restricted to dimers or whether higher-order oligomers may exist (Milligan and Bouvier, 2005). Recent studies on the α_{1b} -adrenoceptor, based on the ability of fragments of this GPCR to self-associate, have

MOL #33035

indicated both transmembrane domain (TMD) I and TMD IV can provide symmetrical interaction interfaces and these observations generated a ‘daisy-chain’ model in which repeating TMD I-I and then TMD IV-IV interactions could potentially produce oligomers rather than simple dimers (Carrillo et al., 2004). One key role that has been suggested for GPCR dimerization/oligomerization is to promote the correct folding and maturation of the receptor (Bulenger et al., 2005) and, subsequently, to allow cell surface delivery. Alterations in GPCR structure can result in retention of the protein in the endoplasmic reticulum (Conn et al., 2006) and hence modification of interfaces involved in GPCR dimerization/oligomerization might be anticipated to limit receptor maturation and cell surface delivery. Although, 2 chromophore fluorescence resonance energy transfer (FRET) imaging (Herman et al., 2004) has become a popular approach to observe GPCR protein-protein interactions in single cells (Milligan and Bouvier, 2005), it is only with the very recent development of 3 chromophore FRET (Galperin et al., 2004) that it has become conceptually possible to image complexes containing at least three polypeptides. Herein we develop and optimize a sequential 3 color FRET imaging approach and use this to demonstrate the presence of oligomeric complexes of the α_{1b} -adrenoceptor in single cells. Introduction of mutations into both TMD I and TMD IV of the α_{1b} -adrenoceptor result in a substantial reduction in the normalized sequential 3 protein FRET signal, indicating alterations in the oligomeric organization. This was accompanied by an inability of the modified receptor to mature correctly, to be delivered to the cell surface and, hence, to function. However,

MOL #33035

use of bi-molecular fluorescence complementation indicated that although these mutations block transport from the endoplasmic reticulum/Golgi they do not inherently eliminate receptor quaternary interactions. Deconstruction of the TMD I + TMD IV receptor mutant indicated the key mutations that alter α_{1b} -adrenoceptor organization are those in TMD IV and that terminal N-glycosylation of the α_{1b} -adrenoceptor (Bjorklof et al., 2002) is not a definitive indication of a fully mature receptor that will be successfully delivered to the plasma membrane.

MATERIALS AND METHODS

Materials

All materials for tissue culture were from Invitrogen (Paisley, UK). [³H]Prazosin was from Perkin Elmer Life Sciences (Boston, MA).

Fluorescent proteins concatamers

Different concatamers containing eCFP-dsRed2, eYFP-dsRed2 or eCFP-eYFP-dsRed2 as single open reading frames were constructed in a similar way as the previously described eCFP-eYFP concatamer (Carrillo et al., 2004). For the construction of the concatamer containing the three fluorescent proteins, the original eCFP-eYFP concatamer subcloned into pcDNA3 (Invitrogen) was digested with KpnI and NotI, allowing the liberation of the eYFP-encoding nucleotide region. Subsequently, eYFP was amplified by PCR from its original vector (Clontech) using as a forward primer: CGGGGTACCATGGTGAGCAAGGGCGAGGAG that

MOL #33035

includes a KpnI restriction site (underlined), and as a reverse primer

CCGGAATTCCTTGTACAGCTCGTCCATGCC where the stop codon had been removed and an EcoRI restriction site had been added. Similarly, dsRed2, a variant of the originally described dsRed1, (Clontech) was amplified using as a forward primer:

CCGGAATTCATGGCCTCTTTGCTGAAGAAC containing an EcoRI restriction site, and as a reverse primer:

TTTTTCCTTTTGCGGCCGCTCAGTTGTGGCCCAGCTTGGA that contains a NotI site. All these PCR products were purified and subsequently digested with the corresponding endonuclease enzymes. Afterwards, the digested PCR products corresponding to eYFP and dsRed2 were ligated to the pcDNA3-eCFP vector obtained after the digestion of eCFP-eYFP concatamer with KpnI and NotI (see above). This ligation resulted in the three fluorescent proteins in tandem within a unique open reading frame. To generate the eCFP-dsRed2 concatamer, eYFP was removed from the original eCFP-eYFP construct by digestion with KpnI and NotI and substituted by dsRed2 containing a KpnI site at the 5' end and a NotI site at the 3' end. Similarly, the eYFP-dsRed2 concatamer was constructed after removing eCFP from the eCFP-dsRed2 construct by digestion with HindIII and KpnI, and subsequent insertion of eYFP without a stop codon containing a HindIII site at 5' end and a KpnI site at 3' end.

α_{1b} -adrenoceptor fusions with fluorescent proteins

Forms of the α_{1b} -adrenoceptor fused to eCFP or eYFP were described in Carrillo et al., 2004. To generate α_{1b} -adrenoceptor C-terminally tagged with dsRed2, we

MOL #33035

removed eCFP from the α_{1b} -adrenoceptor-eCFP construct by digesting with KpnI and NotI endonucleases and inserted a dsRed2 nucleotide sequence containing KpnI and NotI restriction sites at the 5' and 3' ends respectively. In the same way, for bi-molecular fluorescent complementation studies, α_{1b} -adrenoceptor constructs were generated by subcloning the sequence encoding for the N-terminal 172 amino acid fragment or the C-terminal 67 amino acid fragment of eYFP. These two eYFP fragments were selected according to Hu et al., 2002.

Site-directed mutagenesis

To produce amino acid substitutions in the primary structure of the different proteins, site-directed mutagenesis of the encoding nucleotide sequence was performed using the Quick Change[®] II Site-Directed Mutagenesis kit (Stratagene, La Jolla, CA) according to the manufacturer's instructions. The following primers were designed for the mutagenesis of the α_{1b} -adrenoceptor:

GCCATTGTGGGCAACATCGCAGCCATCCTGTCAGTGGCCTGC (forward) and GCAGGCCACTGACAGGATGGCTGCGATGTTGCCACAATGGC (reverse) that substitute Leu and Val at position 65 and 66 respectively in transmembrane domain I by two consecutive Ala (underlined bases); and

AGCAAGGCCATCTTGGCAGCAGCAAGTGTGTGGGTTTTGTCC (forward) and GGACAAAACCCACACACTTGCTGCTGCCAAGATGGCCTTCCT (reverse) that exchange two consecutive Leu residues at positions 166 and 167 in transmembrane domain IV by two consecutive Ala residues.

The same strategy was used to mutate eYFP into a non-fluorescent form by

MOL #33035

substitution of Tyr at position 67 with Cys. In this case the PCR primers used were:
CCACCTTCGGCTGCGGCCTGCAGTG (forward) and
CACTGCAGGCCGCGAGCCGAAGGTGG (reverse).

Transient transfection of HEK293 cells

HEK293 cells were maintained in Dulbecco's modified Eagle's medium supplemented with 0.292 g/l L-glutamine and 10% (v/v) newborn calf serum at 37°C in a 5% CO₂ humidified atmosphere. Cells were grown to 60 to 80% confluence before transient transfection. Transfection was performed using Effectene[®] transfection reagent (Qiagen, Germany) according to the manufacturer's instructions.

Epifluorescence imaging

2-step-FRET microscopy in living cells

HEK293 cells were grown on poly-D-lysine treated coverslips (number 0) and transiently transfected with appropriate eCFP/eYFP/dsRed2 constructs. Coverslips were placed into a microscope chamber containing physiological HEPES-buffered saline solution: (130 mM NaCl, 5 mM KCl, 1 mM CaCl₂, 1 mM MgCl₂, 20 mM HEPES, 10 mM D-glucose, pH 7.4). Cells were then imaged using an inverted Nikon TE2000-E microscope (Nikon Instruments, Melville, NY) equipped with a x40, (NA=1.3), oil-immersion Fluor lens and a cooled digital Cool Snap-HQ CCD camera from Roper Scientific (Photometrics, Tucson, AZ).

Epifluorescence excitation light was generated by an ultra high point intensity 75 W xenon arc Optosource lamp (Cairn Research, Faversham, Kent, UK) coupled to a

MOL #33035

computer controlled Optoscan monochromator (Cairn Research, Faversham, Kent, UK). Monochromator was set to 425/10 nm, 495/9 nm and 580/10 nm for the sequential excitation of eCFP, eYFP and dsRed2 respectively. eCFP, eYFP and dsRed2 excitation light was transmitted through the objective lens using a custom designed 86006 polychroic with 440 DCLP for reflection of UV and violet light (Chroma Inc., Rockingham, VT). eCFP, eYFP and dsRed2 fluorescence emission was controlled via a high-speed filterwheel device (Prior Instruments) containing the following band pass emitters: HQ470/30 nm for eCFP; HQ535/30 nm for eYFP and HQ630/60 nm for dsRed2. This excitation/emission set up made it possible to leave the polychroic in place in the microscope. This enhanced image acquisition and therefore lessened the potential threat of motion. Images were collected using a Cool Snap-HQ digital camera operated in 12-bit mode. Computer control of all electronic hardware and camera acquisition was achieved using Metamorph software (version 6.3.3; Molecular Devices Corp., Downing, PA). The illumination time was 230 ms and binning was set to 2 x 2.

To detect sequential FRET in living cells, six-filter channel combinations were established, (i.e. dsRed2: Ex=580/10 nm, Em=630/60 nm; eYFP: Ex=495/9 nm, Em=535/30 nm; eCFP: Ex=425/10 nm, Em=470/30 nm; eCFP/eYFP/FRET: Ex=425/10 nm, Em=535/30 nm; eCFP/eYFP/DsRed2 FRET: Ex=425/10 nm, Em=630/60 nm; eYFP/dsRed2/FRET: 495/9 nm, Em=630/60 nm), which allowed acquisition of images from all three protein fluorophores and three raw FRET images. These images were used to calculate three corrected FRET images. Metamorph imaging software was used to quantify the FRET images as well as to apply the

MOL #33035

necessary algorithms, pixel by pixel based, to obtain a final image corresponding to the corrected and normalized FRET (see below and Supplementary information).

Determination of bleedthrough coefficients

Bleedthrough coefficients were defined as the ratio between the amount of fluorescence detected in the corresponding FRET filter set (F_x) and the fluorescence detected for each single fluorescent protein at its own filter set (eCFP, eYFP and dsRed2). In order to obtain these coefficients, cells were transfected with each of the fluorescent proteins individually and the fluorescence measurements resulted in the following parameters: $F_{\text{CFP-YFP}}/\text{CFP} = 0.82$, $F_{\text{CFP-YFP}}/\text{YFP} = 0.12$, $F_{\text{YFP-dsRed2}}/\text{YFP} = 0.08$, $F_{\text{YFP-dsRed2}}/\text{dsRed2} = 0.05$, $F_{\text{CFP-dsRed2}}/\text{YFP} = 0.01$, $F_{\text{CFP-dsRed2}}/\text{DsRed2} = 0.04$.

FRET signal correction and normalization

As the fluorescence detected in the FRET channel (raw FRET) comprises not only the actual FRET but also the bleedthrough from the fluorescent proteins expressed, this signal was corrected using the bleedthrough coefficients determined previously. In addition, this corrected FRET was also normalized to generate a final value independent of protein expression levels. For this purpose the following equation: $\text{FRET}^{\text{N}} = \text{raw FRET} / \sum(\text{FP} * \text{B}_x)$ was used, where FP is the intensity of each fluorescent protein involved in the final FRET and B_x is its corresponding bleedthrough coefficient, (i.e. fluorescence intensity in the background corrected FRET channel image divided by the total spillover from the relevant FRET partners). Thus, in the

MOL #33035

absence of energy transfer, FRET^N has a predicted value of 1, while values greater than 1 would reflect the occurrence of FRET.

Hoechst 33342 and RQAPB imaging

Glass coverslips bearing HEK293 cells expressing wild type or mutant versions of the α_{1b} -adrenoceptor were rinsed several times in PBS. Cell nuclei were stained by incubating the cells for 20 min at room temperature (RT), with fresh PBS containing the nuclear DNA-binding dye Hoechst 33342 (10 μ g/ml). After 20 min, cells were washed 3-4 times with PBS and re-incubated, (RT), for 70-90 min with fresh PBS supplemented with 10 nM of the red fluorescent α_1 -AR antagonist ligand RQAPB (Pediani et al., 2005). Using the epifluorescence microscope system, Hoechst 33342 and RQAPB were sequentially detected using the appropriate excitation wavelength of light, beam splitter (BS) and emitter, (i.e. Hoechst: Ex=355 nm, BS=400 DCLP, Em=470/30 nm; RQAPB: Ex=550 nm, BS=Q570LP, Em=610/75 nm). Sequential images (no binning) were collected and exposure to excitation light was 150-200 ms/image. Metamorph imaging software was used for image data processing.

[Ca²⁺]_i ratio imaging

HEK293 cells were transfected with FLAG-Leu⁶⁵Ala, Val⁶⁶Ala, Leu¹⁶⁶Ala, Leu¹⁶⁷Ala α_{1b} -adrenoceptor-eCFP or FLAG- α_{1b} -adrenoceptor-eYFP. After 24 h, cells were harvested, mixed and plated onto coverslips where they grew for an additional 24 h prior to experimentation. Transfected cells were loaded with the Ca²⁺-sensitive dye

MOL #33035

Fura-2 AM, (1.5 μM), by incubation (30 min; 37°C) under reduced light in DMEM growth medium. Using the epifluorescence microscope system, loaded cells were essentially illuminated, excited and imaged as previously described above. Optoscan monochromator was used to rapidly alternate the excitation wavelength between 340 and 380 nm and to control the excitation band pass (340 nm: band pass = 10 nm; 380 nm: band pass = 8 nm). Fura-2 fluorescence emission at 510 nm was monitored using a Cool Snap-HQ digital CCD camera. MetaFluor imaging software was used for control of all electronic hardware and image data processing. Sequential images (3×3 binning) were collected every 2 s, exposure to excitation light was 100 ms/image, and all experiments were undertaken in HEPES buffered saline solution, (composition detailed above).

[Ca²⁺]_i image analysis

Ratio images were presented in MetaFluor intensity-modulated display mode, which associates the colour hue with the excitation ratio value and the intensity of each hue with the source image brightness. Background fluorescence was subtracted from each raw image as follows: a region of interest (ROI) was manually drawn in a region of no fluorescence adjacent to the fluorescent cells in the 380 nm channel image, then selected and transferred to the matched image acquired at 340 nm. The background amount was then subtracted from each pixel in each channel. Background subtracted images were then used for calculating the 340/380 nm ratio of each pixel which was used to indicate changes in $[\text{Ca}^{2+}]_i$. After determination of the upper and lower

MOL #33035

thresholds, the ratio value of each pixel was associated with one of the 24 hues from blue (low $[Ca^{2+}]_i$) to red (high $[Ca^{2+}]_i$). Pooled average intensity-modulated display ratio intensity values measured from single cells were expressed as the mean of at least 10 cells with the vertical lines representing S.E. of mean.

Immunocytochemistry fluorescence

Cells grown on coverslips and expressing the appropriate receptor fusion protein were fixed in 4% paraformaldehyde in PBS containing 5% sucrose for 10 min at RT. When indicated, cells were permeabilized for 10 min in TM buffer (0.15% Triton X-100 and 3% non-fat milk in PBS) otherwise the blocking step was performed avoiding the detergent (3% non-fat milk in PBS). Cells were incubated with a rabbit anti-FLAG polyclonal antibody (1:100, Sigma-Aldrich, UK) for 1 h at room temperature and then washed twice with PBS. Cells were then incubated for a further 1 h with an Alexa594-conjugated anti-rabbit antiserum (1:400) (Molecular Probes, Eugene, OR). After washing with PBS, coverslips were mounted onto glass slides and viewed using the epifluorescence microscope. For detection of c-myc- α_{1b} -adrenoceptor-Tyr⁶⁷Cys-eYFP, the same procedure was followed but using a rabbit anti-c-myc polyclonal antiserum (1:100, Cell Signaling Technology Inc., Beverly, MA).

Western blotting

After heating samples at 65°C for 15 min, both cell membrane samples and cell lysates were subjected to SDS-PAGE analysis using 4 to 12% Bis-Tris gels (Nu-PAGE; Invitrogen) and MOPS buffer. After electrophoresis, proteins were transferred

MOL #33035

onto nitrocellulose membranes that were incubated in 5% non-fat milk and 0.1% Tween 20/PBS solution at room temperature on a rotating shaker for 2 h to block non-specific binding sites. The membrane was incubated overnight with a polyclonal anti-GFP antiserum and detected using a horseradish peroxidase-linked anti-goat IgG secondary antiserum (GE Healthcare). Immunoblots were developed by application of enhanced chemiluminescence solution (Pierce Chemical, Rockford, IL).

Endoglycosidase treatment

Endoglycosidase treatment was carried out on membrane preparations using PNGase F (Roche Diagnostics, Germany) at a final concentration of 1 unit/ μ l at room temperature for 14-16 h.

[³H]Prazosin binding studies

Binding assays were initiated by the addition of 15-20 μ g of cell membranes to an assay buffer (50 mM Tris-HCl, 100 mM NaCl, 3 mM MgCl₂, pH 7.4) containing [³H]prazosin (0.02-1 nM in saturation assays and 0.4 nM for competition assays) in the absence or presence of increasing concentrations of phenylephrine. Non-specific binding was determined in the presence of 100 μ M phentolamine. Reactions were incubated for 60 min at 30°C, and bound ligand was separated from free ligand by vacuum filtration through GF/B filters (Semat, St. Albans, Hertsfordshire, UK). The filters were washed twice with assay buffer, and bound ligand was estimated by liquid scintillation spectrometry.

MOL #33035

RESULTS

Development of sequential 3 color FRET imaging using chromophore concatamers

Previous studies based on the ability of co-expressed fragments of the hamster α_{1b} -adrenoceptor to interact (Carrillo et al., 2004), allowed us to propose a model for the organization of this GPCR that consists of a chain of polypeptide monomers linked by alternating symmetrical TMD I-TMD I and TMD IV-TMD IV interactions (Figure 1). To establish appropriate conditions and algorithms to monitor the transfer of energy within oligomeric complexes involving at least three polypeptides in living cells we generated a concatamer (Figure 2A) in which the dsRed2 fluorescent protein (Erickson et al., 2003) (a variant of the original dsRed1 from the reef coral *Discosoma* that has improved solubility and a reduced tendency to form aggregates) was linked in-frame to the C-terminus of a single open-reading frame containing the sequences of both the enhanced cyan (eCFP) and enhanced yellow (eYFP) variants of the *Aequoria victoria* green fluorescent protein. We have previously used the eCFP-eYFP single open reading frame (Figure 2A) as a positive control for imaging conventional, CFP to YFP, 2 protein FRET (Carrillo et al., 2004). Furthermore, concatamers of all possible combinations of two of the three individual fluorescent proteins used in these studies (Figure 2A) were also generated and analyzed (see Materials and Methods) to account for possible spill-over and bleedthrough. When expressed in HEK293 cells the 3 protein eCFP-eYFP-dsRed2 concatamer was distributed evenly throughout the cytoplasm but excluded from the nucleus (Figure 2B(A)). Excitation of the eCFP element of this concatamer with 430 nm light (monochromator set to 425/10 nm) (Figure 2C) followed by cell imaging and appropriate correction for bleedthrough and

MOL #33035

spill-over between channels (see Materials and Methods and Supplementary data for details) allowed detection of eCFP to eYFP FRET (Figure 2B(A₄)) as well as eCFP to dsRed2 FRET (Figure 2B(A₆)). Excitation of the eYFP component of the concatamer with 495 nm (monochromator set to 495/9 nm) light allowed detection of eYFP to dsRed2 FRET (Figure 2B(A₅)).

eCFP to dsRed2 FRET may represent a combination of direct eCFP-dsRed2 FRET as well as sequential eCFP-eYFP-dsRed2 FRET (Figure 2C) but only sequential 3 protein FRET can provide information on oligomeric rather than dimeric interactions. To establish the component of eCFP to dsRed2 FRET signal reflecting direct 2 protein eCFP to dsRed2 versus sequential eCFP to eYFP to dsRed2, 3 protein FRET (Figure 2C), a Tyr⁶⁷Cys mutation, known to ablate fluorescence, was introduced into the eYFP segment of the concatamer (Figure 2A). When this concatamer, in which the distance between and relative orientation of eCFP and dsRed2 is unchanged from the wild type concatamer, was expressed in HEK293 cells, both the eCFP and dsRed2 elements retained fluorescence (Figure 2B(B₁) and 2B(B₃)) but, as anticipated, minimal signals were obtained in each of the eCFP to eYFP, eCFP to dsRed2 and eYFP to dsRed2 FRET channels (Figure 2B (B₄, B₅, B₆)). Because Tyr⁶⁷Cys YFP is not fluorescent (Figure 2B(B₂)) then the minimal signal obtained at 630 nm (Em=630/60 nm) after excitation of cells expressing the eCFP-Tyr⁶⁷Cys YFP-dsRed2 concatamer at 430 nm must represent direct eCFP to dsRed2 FRET and therefore the difference in signal obtained at 630 nm when using eCFP-eYFP-dsRed2 and eCFP-Tyr⁶⁷Cys YFP-dsRed2 concatamers represents the true sequential 3 protein FRET signal (Figure 2C, Figure 2D₃). In addition, the possible contribution of an eYFP

MOL #33035

component being transferred to the dsRed2 due to excitation of eYFP by 430 nm light (i.e. as a concomitant of excitation of eCFP) was assessed using the eYFP-dsRed2 two protein concatamer (Figure 2A) but no FRET was detected (data not shown). As a further control we co-transfected cells with isolated forms of each of eCFP, eYFP and dsRed2. All of these three proteins were co-expressed in individual cells (Figure 2B(C₁, C₂, C₃)) and in this case, as well as even distribution throughout the cytoplasm, some nuclear localization was observed. However, as for the eCFP-Tyr⁶⁷Cys YFP-dsRed2 concatamer, negligible FRET signals were obtained in each channel (Figure 2B(C₄, C₅, C₆)) consistent with the concept that the three fluorescent proteins do not have significant inherent affinity for each other and as individual polypeptides were not constrained to be within FRET competent distances.

Quantitation of the extent of normalized eCFP to eYFP and eYFP to dsRed2 two protein FRET as well as eCFP to eYFP to dsRed2, 3 protein FRET (Figure 2D) was achieved by imaging cells expressing various of the 2 protein open-reading frame concatamers (Figure 2A) and the 3 protein concatamers described above, as well as by co-expression of different pairs of the three individual fluorescent proteins. Of central importance for the current studies, with the parameters and corrections employed, a substantially higher value was obtained for eCFP-dsRed2 FRET in cells expressing eCFP-eYFP-dsRed2 than in those expressing the eCFP-Tyr⁶⁷Cys eYFP-dsRed2 concatamer (Figure 2D₃). Because dsRed2 retains some capacity to self-associate we also co-expressed the eCFP-dsRed2 and eYFP-dsRed2 two protein concatamers. No significant sequential 3 protein, or single eCFP to eYFP FRET was recorded (data not

MOL #33035

shown), eliminating the formal possibility that dsRed2 self-association brought all three fluorescent polypeptides into a complex within FRET competent distances. These results demonstrate the ability to image and quantitate sequential eCFP to eYFP to dsRed2, 3 protein FRET in individual living cells and hence to generate a system that can be applied to detect the presence of at least three appropriately tagged polypeptides in a quaternary structure complex, to define the appropriate background for subtraction and to eliminate any contribution of direct eCFP-dsRed2 FRET to 3 protein FRET datasets.

The α_{1b} -adrenoceptor is able to form oligomers and the organizational structure is altered by combined mutations in TMD I and TMD IV

We next employed 3 protein FRET to garner support for the presence of oligomeric rather than dimeric α_{1b} -adrenoceptor organization in single, transfected cells and to explore the molecular basis for this. Co-expression of each of C-terminally tagged eCFP, eYFP and dsRed2 forms of the α_{1b} -adrenoceptor (Figure 3A) in HEK293 cells followed by excitation at 430 nm resulted in each of eCFP to eYFP, and eCFP to dsRed2 FRET signals (Figure 3B(A)). Excitation with 495 nm light resulted in eYFP to dsRed2 FRET (Figure 3B(A)). With co-expression of α_{1b} -adrenoceptor-eCFP, α_{1b} -adrenoceptor-Tyr⁶⁷Cys eYFP and α_{1b} -adrenoceptor-dsRed2, eCFP to dsRed2 FRET was virtually eliminated (Figure 3B, C). As any eCFP to dsRed2 FRET signal obtained in the presence of α_{1b} -adrenoceptor-Tyr⁶⁷Cys eYFP must represent direct eCFP to dsRed2 FRET then subtraction of this value from that obtained following co-expression of the eCFP, eYFP and dsRed2 tagged forms of the receptor provided the

MOL #33035

true sequential 3 protein FRET, GPCR oligomer signal (Figure 3C). The lack of eCFP-dsRed2 FRET signal in the presence of α_{1b} -adrenoceptor-Tyr⁶⁷Cys eYFP did not reflect lack of expression of this construct. Although not fluorescent, incorporation of an N-terminal c-myc epitope tag into the construct allowed immunological detection of expression of α_{1b} -adrenoceptor-Tyr⁶⁷Cys eYFP with the same pattern of distribution as α_{1b} -adrenoceptor-eCFP and α_{1b} -adrenoceptor-dsRed2 (Figure 3D). Furthermore, in the quantified data, FRET signals were normalized (see Material and Methods and Supplemental data) to take account of any variation in construct expression levels. As the difference in eCFP to dsRed2 FRET in these cases must correspond to sequential eCFP to eYFP to dsRed2, 3 protein FRET these results demonstrate that at least a proportion of these receptors were within an oligomeric complex comprising at least three receptor monomers within FRET competent distances.

Based on our prediction of key TMD helices for oligomerization of the α_{1b} -adrenoceptor (Carrillo et al., 2004) and the bio-informatic identification of the role of specific amino acids in both TMD I and TMD IV in the quaternary structure of the CCR5 receptor (Hernanz-Falcon et al., 2004; De Juan et al., 2005) we generated a Leu⁶⁵Ala, Val⁶⁶Ala, Leu¹⁶⁶Ala, Leu¹⁶⁷Ala α_{1b} -adrenoceptor. This contains point mutations in hydrophobic residues in both TMD I (Leu⁶⁵Ala, Val⁶⁶Ala) and TMD IV (Leu¹⁶⁶Ala, Leu¹⁶⁷Ala) (Figure 3A) that are similar to those modified by Hernanz-Falcon et al., (2004), and reported to eliminate 2 protein FRET signals corresponding to protein-protein interactions for the CCR5 receptor. Co-expression of C-terminally

MOL #33035

eCFP, eYFP and dsRed2 tagged forms of the Leu⁶⁵Ala, Val⁶⁶Ala, Leu¹⁶⁶Ala, Leu¹⁶⁷Ala α_{1b} -adrenoceptor resulted in a substantial decline of normalized eCFP-dsRed2 FRET (Figure 3B(B₆), Figure 3C) when compared with wild type α_{1b} -adrenoceptor, although there was no reduction in expression of the mutants based on the fluorescence corresponding to the eCFP, eYFP or dsRed2 tags (Figure 3B (A₁-A₃ versus B₁-B₃)). Applying the direct eCFP-dsRed2 FRET correction provided by the Tyr⁶⁷Cys eYFP mutant, sequential 3 protein eCFP to eYFP to dsRed2 FRET was reduced by 56% ($p < 0.05$) in cells expressing the tagged forms of Leu⁶⁵Ala, Val⁶⁶Ala, Leu¹⁶⁶Ala, Leu¹⁶⁷Ala α_{1b} -adrenoceptor (Figure 3C). These results indicate that the introduced mutations reduced the proximity and/or altered the orientation of the fluorescent proteins linked to the mutant α_{1b} -adrenoceptor and hence are consistent with mutations causing disruption of the organizational structure of the α_{1b} -adrenoceptor oligomeric complex.

The Leu⁶⁵Ala, Val⁶⁶Ala, Leu¹⁶⁶Ala, Leu¹⁶⁷Ala α_{1b} -adrenoceptor fails to mature, is not delivered to the cell surface and does not signal

A key question in understanding the importance of GPCR quaternary structure is whether modulation of protein-protein interactions can modify receptor maturation and/or cell surface delivery and therefore function (Bulenger et al., 2005). At least in some cell lines and native tissues α_1 -adrenoceptor subtypes are known to recycle to and from the plasma membrane via endosomal pools both rapidly and constitutively and therefore, at steady-state, a large proportion of these GPCRs is inside the cell rather than at the plasma membrane (Morris et al., 2004, Pediani et al., 2005). When

MOL #33035

comparing the distribution pattern of N-terminally epitope-tagged forms of wild type α_{1b} -adrenoceptor-eYFP with that of Leu⁶⁵Ala, Val⁶⁶Ala, Leu¹⁶⁶Ala, Leu¹⁶⁷Ala α_{1b} -adrenoceptor-eYFP in non-permeabilized and permeabilized transfected HEK293 cells, cell surface, anti-epitope tag staining in non-permeabilized cells could be shown for the wild type α_{1b} -adrenoceptor (Figure 4A(A₂)) but not for Leu⁶⁵Ala, Val⁶⁶Ala, Leu¹⁶⁶Ala, Leu¹⁶⁷Ala α_{1b} -adrenoceptor (Figure 4A(C₂)). Furthermore, α_1 -adrenoceptors are able to bind and internalize the ligand BODIPY-FL prazosin (QAPB) only if they had previously reached the cell surface (Pediani et al., 2005). QAPB displays significant fluorescence only when bound to receptor. A form of QAPB (RQAPB) that displays red fluorescence when bound to α_1 -adrenoceptor subtypes (Pediani et al., 2005) was provided to cells expressing wild type α_{1b} -adrenoceptor-eYFP. Living cells subsequently displayed intracellular red fluorescence (Figure 4B(A₃)). This did not occur in cells expressing Leu⁶⁵Ala, Val⁶⁶Ala, Leu¹⁶⁶Ala, Leu¹⁶⁷Ala α_{1b} -adrenoceptor-eYFP (Figure 4B(B₃)). This was not a reflection that Leu⁶⁵Ala, Val⁶⁶Ala, Leu¹⁶⁶Ala, Leu¹⁶⁷Ala α_{1b} -adrenoceptor is simply denatured and is inherently unable to bind antagonist ligands. However, although direct measures of expression levels based on fluorescence corresponding to α_{1b} -adrenoceptor-eYFP and Leu⁶⁵Ala, Val⁶⁶Ala, Leu¹⁶⁶Ala, Leu¹⁶⁷Ala α_{1b} -adrenoceptor-eYFP (Figure 5A) indicated that the mutations did not hinder protein expression, the capacity of Leu⁶⁵Ala, Val⁶⁶Ala, Leu¹⁶⁶Ala, Leu¹⁶⁷Ala α_{1b} -adrenoceptor-eYFP to bind [³H]prazosin was substantially reduced (wild type = 2.02 ± 0.37; Leu⁶⁵Ala, Val⁶⁶Ala, Leu¹⁶⁶Ala, Leu¹⁶⁷Ala α_{1b} -adrenoceptor = 0.36 ± 0.03

MOL #33035

pmol/mg membrane protein, means \pm SEM, n = 5)) (Figure 5B). However, the affinity of [³H]prazosin for the Leu⁶⁵Ala, Val⁶⁶Ala, Leu¹⁶⁶Ala, Leu¹⁶⁷Ala α_{1b} -adrenoceptor-eYFP binding sites it was able to label was not reduced (K_d wild type = 85 ± 13 pM; Leu⁶⁵Ala, Val⁶⁶Ala, Leu¹⁶⁶Ala, Leu¹⁶⁷Ala α_{1b} -adrenoceptor-eYFP = 33 ± 3 pM). Equally, competition studies employing a single concentration of [³H]prazosin and varying concentrations of RQAPB demonstrated that the affinity of RQAPB was actually slightly higher for the Leu⁶⁵Ala, Val⁶⁶Ala, Leu¹⁶⁶Ala, Leu¹⁶⁷Ala α_{1b} -adrenoceptor ($pK_i = 8.85 \pm 0.18$) than for the wild type α_{1b} -adrenoceptor ($pK_i = 8.33 \pm 0.02$).

Interestingly, when samples expressing wild type α_{1b} -adrenoceptor-eYFP and Leu⁶⁵Ala, Val⁶⁶Ala, Leu¹⁶⁶Ala, Leu¹⁶⁷Ala α_{1b} -adrenoceptor-eYFP were resolved by SDS-PAGE and immunoblotted with an anti-GFP antiserum, the patterns were distinct. Whilst Leu⁶⁵Ala, Val⁶⁶Ala, Leu¹⁶⁶Ala, Leu¹⁶⁷Ala α_{1b} -adrenoceptor-eYFP migrated predominantly as a single band of some 75 kDa, wild type α_{1b} -adrenoceptor-eYFP was represented by a mixture of 75 kDa and 105 kDa polypeptides (Figure 5C). Previous studies have indicated these to represent the core glycosylated (lower molecular mass) precursor form and mature (higher molecular mass) form of the receptor (Bjorklof *et al.*, 2002). In accord with this, treatment of membranes expressing wild type α_{1b} -adrenoceptor-eYFP with N-glycosidase F eliminated the 105 kDa band, with all the immunoreactivity now migrating with apparent M_r between 70-75 kDa (Figure 5D).

To further explore if the mutations introduced into TMD I and TMD IV eliminated α_{1b} -adrenoceptor protein-protein interactions and quaternary structure we employed

MOL #33035

bi-molecular fluorescence complementation (Kerppola, 2006). When eYFP is split into N-terminal 172 amino acid and C-terminal 67 amino acid fragments neither displays inherent auto-fluorescence. However, if they are linked to polypeptides that form a protein complex this can be sufficient to bring the two fragments of eYFP into proximity and allow partial reformation of the fluorescent protein chromophore (Kerppola, 2006). When N-terminally FLAG-tagged forms of the α_{1b} -adrenoceptor with either N-172-eYFP or C-67-eYFP fragments linked to the receptor C-terminus were expressed individually in HEK293 cells, no yellow auto-fluorescence was observed (Figure 6, A₁, B₁), although successful expression of the constructs could be shown via anti-FLAG immunocytochemistry (Figure 6A₂, B₂). However, following co-expression of these two constructs eYFP fluorescence was generated (Figure 6C₁). This dimeric/oligomeric α_{1b} -adrenoceptor complex was able to reach the surface of transfected HEK293 cells because addition of RQAPB to these cells resulted in the appearance of red fluorescence at the cell surface and inside the cells (Figure 7). Merging of the fluorescent signals corresponding to the complemented eYFP, and hence the dimeric/oligomeric α_{1b} -adrenoceptor, and RQAPB resulted in a strong overlap correlation co-efficient ($r^2 = 0.84$) (Figure 7, A₄) consistent with RQAPB being bound to the receptor when it was at the plasma membrane followed by internalization and cycling of the α_{1b} -adrenoceptor dimer/oligomer with the ligand still bound. By contrast, when c-myc-Leu⁶⁵Ala, Val⁶⁶Ala, Leu¹⁶⁶Ala, Leu¹⁶⁷Ala α_{1b} -adrenoceptor-N-172-eYFP and FLAG-Leu⁶⁵Ala, Val⁶⁶Ala, Leu¹⁶⁶Ala, Leu¹⁶⁷Ala α_{1b} -adrenoceptor-C-67-eYFP were co-expressed, although fluorescence complementation was achieved, indicating the two forms of the receptor were in proximity, the

MOL #33035

complemented eYFP signal was restricted entirely to a perinuclear, endoplasmic reticulum/Golgi location and the addition of RQAPB failed to generate red fluorescence (Figure 7, B₃), consistent with the premise that the mutant form of the receptor had never reached the cell surface.

If only the oligomeric wild type α_{1b} -adrenoceptor matures and is able to reach the cell surface then only the wild type would be anticipated to generate signals in response to agonist ligands. Cells expressing either wild type α_{1b} -adrenoceptor-eYFP or Leu⁶⁵Ala, Val⁶⁶Ala, Leu¹⁶⁶Ala, Leu¹⁶⁷Ala α_{1b} -adrenoceptor-eCFP were plated onto different sections of a single coverslip, imaged (Figure 8A) and loaded with the Ca²⁺ indicator dye FURA-2. In cells expressing wild type α_{1b} -adrenoceptor-eYFP, addition of the α -adrenoceptor agonist phenylephrine resulted in elevation of intracellular [Ca²⁺] (Figures 8B, 8C). By contrast, no such signal was produced in equivalent cells expressing Leu⁶⁵Ala, Val⁶⁶Ala, Leu¹⁶⁶Ala, Leu¹⁶⁷Ala α_{1b} -adrenoceptor-eCFP (Figure 8B, 8C). This did not reflect that expression of Leu⁶⁵Ala, Val⁶⁶Ala, Leu¹⁶⁶Ala, Leu¹⁶⁷Ala α_{1b} -adrenoceptor-eCFP somehow ablated the potential for receptor-mediated [Ca²⁺] elevation. In cells expressing either wild type or Leu⁶⁵Ala, Val⁶⁶Ala, Leu¹⁶⁶Ala, Leu¹⁶⁷Ala α_{1b} -adrenoceptor, subsequent to challenge with phenylephrine, addition of ATP to activate the endogenously expressed P2Y purinoceptor population resulted in equivalent elevations of intracellular [Ca²⁺] (Figure 8C). Again, the lack of capacity of Leu⁶⁵Ala, Val⁶⁶Ala, Leu¹⁶⁶Ala, Leu¹⁶⁷Ala α_{1b} -adrenoceptor to respond to phenylephrine did not reflect an inherent inability to bind the agonist ligand. Phenylephrine was actually substantially more potent in competing for the binding of [³H]prazosin in membrane preparations

MOL #33035

of cells expressing Leu⁶⁵Ala, Val⁶⁶Ala, Leu¹⁶⁶Ala, Leu¹⁶⁷Ala α_{1b} -adrenoceptor than the wild type receptor (Figure 9).

Although we were unable to detect Leu⁶⁵Ala, Val⁶⁶Ala, Leu¹⁶⁶Ala, Leu¹⁶⁷Ala α_{1b} -adrenoceptor at the cell surface, we wished to ascertain if small amounts of the mutant might reach the cell surface and the limits of detectability. Initially, we transfected HEK293 cells with varying amounts of cDNA corresponding to the wild type α_{1b} -adrenoceptor-eYFP construct, generated membranes and performed [³H]prazosin binding studies. A 4 fold reduction in cDNA amount translated to an approximately 10 fold reduction in [³H]prazosin binding levels (Figure 10A). Parallel studies directly measured eYFP fluorescence and provided similar conclusions (Figure 10B). Scaling the amounts of cDNA used to transfect cells for [Ca²⁺] mobilization imaging/assays showed that phenylephrine-mediated elevation of [Ca²⁺] was easily detected, even with amounts of cDNA that resulted in an inability to resolve total from non-specific [³H]prazosin binding and hence is at the limit of receptor detection (Figure 10C). However, [Ca²⁺] elevation did require some level of wild type α_{1b} -adrenoceptor-eYFP expression because no response was observed to phenylephrine in mock-transfected cells (Figure 10C). As such, the inability of phenylephrine to cause elevation of intracellular [Ca²⁺] in cells expressing the Leu⁶⁵Ala, Val⁶⁶Ala, Leu¹⁶⁶Ala, Leu¹⁶⁷Ala α_{1b} -adrenoceptor implies that if any of this mutant reaches the cell surface it must be in vanishingly small amounts.

In a number of cases, receptor mutants that cannot escape the endoplasmic reticulum/Golgi apparatus after synthesis can act as ‘dominant negatives’ and limit cell surface delivery of a co-expressed, wild type version of the same receptor. This is

MOL #33035

both relevant to a number of human diseases and has provided evidence for a requirement for protein-protein interactions between GPCR monomers prior to cell surface delivery (Bulenger et al., 2005). As the bi-molecular fluorescence complementation studies had shown that the Leu⁶⁵Ala, Val⁶⁶Ala, Leu¹⁶⁶Ala, Leu¹⁶⁷Ala α_{1b} -adrenoceptor was still able to self-dimerize/oligomerize to some extent we asked whether this mutant would prevent cell surface delivery of wild type α_{1b} -adrenoceptor. HEK293 cells were transfected to express either c-myc- α_{1b} -adrenoceptor-Y⁶⁷C-eYFP alone (Figure 11A) or together with FLAG-Leu⁶⁵Ala, Val⁶⁶Ala, Leu¹⁶⁶Ala, Leu¹⁶⁷Ala α_{1b} -adrenoceptor-eYFP in a 1:3 ratio (Figures 11B, C). Immunocytochemistry using an anti-c-myc antibody and a secondary antibody conjugated to Alexa594 in non-permeabilized cells detected the wild type receptor at the cell surface in the absence of the mutant (Figure 11A), whilst cell surface wild type α_{1b} -adrenoceptor was undetectable in cells co-expressing FLAG-Leu⁶⁵Ala, Val⁶⁶Ala, Leu¹⁶⁶Ala, Leu¹⁶⁷Ala α_{1b} -adrenoceptor-eYFP (Figure 11B), the expression of which was detected by monitoring eYFP fluorescence (Figure 11B). Anti-c-myc immunocytochemistry in permeabilized cells co-expressing the wild type and mutant forms of the receptor confirmed the expression and intracellular location of c-myc- α_{1b} -adrenoceptor-Y⁶⁷C-eYFP (Figure 11C), whilst merging of the anti-c-myc and eYFP signals confirmed the co-distribution of the two forms (Figure 11C). As a control for these studies we transiently transfected cells with FLAG-Leu⁶⁵Ala, Val⁶⁶Ala, Leu¹⁶⁶Ala, Leu¹⁶⁷Ala α_{1b} -adrenoceptor-eYFP and c-myc-CXCR1 because we have previously demonstrated negligible interactions between CXCR1 and α_{1b} -

MOL #33035

adrenoceptors (Wilson et al., 2005). The presence of FLAG-Leu⁶⁵Ala, Val⁶⁶Ala, Leu¹⁶⁶Ala, Leu¹⁶⁷Ala α_{1b} -adrenoceptor-eYFP failed to interfere with cell surface delivery of anti-c-myc immunoreactivity corresponding to the CXCR1 receptor (Figure 11D).

The capacity to be terminally N-glycosylated does not determine cell surface delivery and function of the α_{1b} -adrenoceptor

To attempt to ascertain individual contributions of the TMD I and TMD IV mutations to the phenotype of the combined Leu⁶⁵Ala, Val⁶⁶Ala, Leu¹⁶⁶Ala, Leu¹⁶⁷Ala α_{1b} -adrenoceptor, both Leu⁶⁵Ala, Val⁶⁶Ala α_{1b} -adrenoceptor and Leu¹⁶⁶Ala, Leu¹⁶⁷Ala α_{1b} -adrenoceptor mutants were constructed. Following addition of each of eCFP, eYFP, or dsRed2 to the C-terminal tail of each mutant, these potentially FRET competent forms were co-expressed in HEK293 cells and 3-FRET studies performed. The sequential eCFP to eYFP to dsRed2 3-FRET signal for the Leu⁶⁵Ala, Val⁶⁶Ala α_{1b} -adrenoceptor was indistinguishable from the wild type α_{1b} -adrenoceptor (Figure 12), whilst the Leu¹⁶⁶Ala, Leu¹⁶⁷Ala α_{1b} -adrenoceptor mutant generated a reduced 3-FRET signal that was not statistically different from the reduction in 3-FRET produced by the Leu⁶⁵Ala, Val⁶⁶Ala, Leu¹⁶⁶Ala, Leu¹⁶⁷Ala α_{1b} -adrenoceptor (Figure 12). Interestingly, however, although both the Leu⁶⁵Ala, Val⁶⁶Ala α_{1b} -adrenoceptor and the Leu¹⁶⁶Ala, Leu¹⁶⁷Ala α_{1b} -adrenoceptor failed to be delivered to the plasma membrane (Figure 13A, B), immunoblotting studies demonstrated that both these forms were able to mature into the 105 kDa form of the receptor and the ratios of

MOL #33035

105kDa to 75kDa species were not different from the wild type α_{1b} -adrenoceptor (Figure 13C).

DISCUSSION

The lack of ability to discriminate between dimeric and oligomeric GPCR organization has generally resulted in these terms being used interchangeably (Milligan, 2006). Although combined immune capture and co-immunoprecipitation of three differently epitope-tagged and co-expressed forms of the M2 muscarinic acetylcholine receptor (Park and Wells, 2004) was certainly consistent with oligomeric interactions, this approach has not been employed frequently and is limited by the same issues that have dogged analysis of co-immunoprecipitation of pairs of GPCRs (Milligan and Bouvier, 2005). Many recent efforts to explore GPCR quaternary structure have, therefore, centred on the use of either bioluminescence or fluorescence resonance energy transfer with eYFP acting as energy acceptor for light produced either by excitation of eCFP or oxidation of a substrate by a luciferase (Milligan and Bouvier, 2005). Bioluminescence resonance energy transfer techniques are not currently compatible with cell imaging and although FRET techniques are, only a limited number of studies have attempted to expand 2 protein FRET imaging to 3 protein FRET imaging (Galperin et al., 2004). As well as the inherently small signals anticipated in these studies this reflects, in part, the necessity for custom filter sets to define and optimally limit spill-over of emitted light into the individual FRET channels and requirements to define that eCFP to red fluorescent protein FRET signals actually represent sequential energy transfer between appropriate resonance

MOL #33035

energy transfer pairings. As previously described by Galperin et al., 2004, we developed sequential 3-FRET and optimized filter sets by employing concatamers of three fluorescent proteins that are FRET compatible. We also employed the Tyr⁶⁷Cys eYFP mutation to estimate direct eCFP-dsRed2 FRET versus sequential eCFP-eYFP-dsRed2 FRET. Finally, to generate data with sufficiently low co-efficient of variation to allow statistically significant differences in sequential 3 FRET signals to be recorded for oligomers of the wild type and mutant α_{1b} -adrenoceptor constructs required development of a new modified ratio method for FRET quantification we term RFRET. This greatly improved the co-efficient of variation in both our own data and published data from others compared to previous FRET quantification algorithms (see Supplemental data).

With such technical information in place we were able to demonstrate sequential 3 protein FRET between appropriately tagged forms of the α_{1b} -adrenoceptor, confirming our previous prediction that oligomers of this GPCR, rather than only dimers, would exist (Carrillo et al., 2004). As we had also predicted that this would reflect, at least in part, both TMD I-TMD I and TMD IV-TMD IV interactions we used mutagenesis to test this hypothesis. Interestingly, in studies on the chemokine CCR5 receptor Hernanz-Falcon et al., (2004) reported using bio-informatics to predict amino acids in both TMD I and TMD IV important for receptor 'dimerization' (de Juan et al., 2005) and demonstrated a loss of 2 protein FRET signals, potentially consistent with a lack of interaction following mutation. The studies of Hernanz-Falcon et al., (2004) have attracted considerable interest. Although the mutants we introduced into the α_{1b} -adrenoceptor were based, in part, on alignments with the

MOL #33035

CCR5 receptor, the results we have produced are quite different. For example, Hernanz-Falcon et al., (2004) reported a complete loss of 2 protein FRET signal. We observe only a partial loss of sequential 3 protein FRET. This may be for a number of reasons. Firstly, these single point mutations in TMDs appear to be insufficient to fully disassemble a dimer/oligomer. Secondly, in our previous analysis of the oligomeric potential of the α_{1b} -adrenoceptor we also noted further, non-symmetrical, interactions between TMD I and/or II with TMD V and/or VI (Carrillo et al., 2004) and concluded these might allow generation of a structure akin to the ‘arrays of dimers’ noted for murine rhodopsin (Fotiadis et al., 2004). Interactions within an α_{1b} -adrenoceptor oligomer may, therefore, be only partially disrupted by point mutations in TMDs I and IV. It is also important to note that the biophysical basis of any resonance energy transfer study is dependent upon both distance between the energy donor and acceptor species and their relative orientation (Pfleger and Edine, 2006). Interestingly, Hernanz-Falcon et al., (2004) also reported the mutated CCR5 receptor that was unable to ‘dimerize’ was delivered effectively to the cell surface. Again our observations are different. The Leu⁶⁵Ala, Val⁶⁶Ala, Leu¹⁶⁶Ala, Leu¹⁶⁷Ala α_{1b} -adrenoceptor was completely unable to reach the cell surface. This may reflect growing evidence that GPCR dimers/oligomers form during protein synthesis (Salahpour et al., 2004; Wilson et al., 2005) and that this is required for cell surface delivery.

In certain cases an inability to reach the cell surface reflects an inability of receptors to become fully N-glycosylated and hence pass cellular quality control (Petaja-Repo et al., 2002; Pietila et al., 2005). We show herein that Leu⁶⁵Ala, Val⁶⁶Ala, Leu¹⁶⁶Ala,

MOL #33035

Leu¹⁶⁷Ala α_{1b} -adrenoceptor is indeed unable to mature and become fully N-glycosylated. As well as relying on the capacity in intact cells to detect an epitope tag added to the N-terminus of the receptor that is expected to be on the extracellular face of the cell if the receptor was successfully delivered to the plasma membrane, we also employed a range of other techniques to determine if the various forms of the α_{1b} -adrenoceptor were able to reach the cell surface. Bi-molecular fluorescence complementation demonstrated that although the Leu⁶⁵Ala, Val⁶⁶Ala, Leu¹⁶⁶Ala, Leu¹⁶⁷Ala α_{1b} -adrenoceptor still maintained quaternary structure, it remained in the endoplasmic reticulum/Golgi. α_1 -adrenoceptors recycle rapidly in cells without the presence of an agonist ligand (Pediani et al., 2005) and hence at steady-state a substantial fraction of the wild type receptor is inside the cells. However, treatment of cells expressing bi-molecular fluorescence complementation-competent forms of the wild type α_{1b} -adrenoceptor with the fluorescent α_1 -adrenoceptor ligand RQAPB confirmed that the receptor had travelled to the cell surface to bind and internalize the ligand whilst no interaction of RQAPB could be detected for Leu⁶⁵Ala, Val⁶⁶Ala, Leu¹⁶⁶Ala, Leu¹⁶⁷Ala α_{1b} -adrenoceptor, indicating that this mutant had never been at the cell surface.

The Leu⁶⁵Ala, Val⁶⁶Ala, Leu¹⁶⁶Ala, Leu¹⁶⁷Ala α_{1b} -adrenoceptor also displayed unexpected pharmacological characteristics. Measures of protein expression and amount based on the fluorescence of attached tags clearly demonstrated the Leu⁶⁵Ala, Val⁶⁶Ala, Leu¹⁶⁶Ala, Leu¹⁶⁷Ala α_{1b} -adrenoceptor to be expressed as well as wild type α_{1b} -adrenoceptor. However, this would not have been the conclusion if analysis had been restricted to [³H]antagonist binding studies, where the capacity, but not affinity,

MOL #33035

of Leu⁶⁵Ala, Val⁶⁶Ala, Leu¹⁶⁶Ala, Leu¹⁶⁷Ala α_{1b} -adrenoceptor to bind [³H]prazosin was markedly reduced. Others have reported substantial differences in binding capacity of a single GPCR for different [³H]antagonist ligands and such data has been used to argue for co-operativity between binding sites and hence GPCR quaternary structure (Park et al., 2004; Strange, 2005; Franco et al., 2006). Disruption of quaternary structure might therefore modulate ligand binding capacity. Despite this, Leu⁶⁵Ala, Val⁶⁶Ala, Leu¹⁶⁶Ala, Leu¹⁶⁷Ala α_{1b} -adrenoceptor retained ability to bind the agonist ligand phenylephrine and, indeed, displayed a higher affinity to bind this agonist than the wild type receptor.

A significant number of genetic diseases reflect mutations in genes that result in endoplasmic reticulum/Golgi apparatus retention of the expressed protein. In a number of examples the mutated proteins are GPCRs (Bernier et al., 2004; Ulloa-Aguirre et al., 2004). Interestingly, mutant GPCRs that are expressed but are unable to transit through the endoplasmic reticulum/Golgi apparatus frequently act as ‘dominant negatives’ for cell surface delivery of a co-expressed wild type GPCR (Duvernay et al., 2005) and this may also be directly relevant to physiology and disease as certain GPCR splice variants display this characteristic (Ding et al., 2002). This indicates that effective and correct interactions to form GPCR dimers/oligomers are central to effective cell surface delivery of GPCRs. The Leu⁶⁵Ala, Val⁶⁶Ala, Leu¹⁶⁶Ala, Leu¹⁶⁷Ala α_{1b} -adrenoceptor studied herein was also shown to have such a ‘dominant negative’ effect on the cell surface delivery of the wild type α_{1b} -adrenoceptor.

MOL #33035

Interestingly, when we studied the effect of mutations in either TMD I or TMD IV in isolation, although both the Leu⁶⁵Ala, Val¹⁶⁶Ala and Leu¹⁶⁶Ala, Leu¹⁶⁷Ala forms of the α_{1b} -adrenoceptor were poorly, if at all, delivered to the cell surface, both of these mutants appeared to be terminally N-glycosylated as effectively as the wild type α_{1b} -adrenoceptor. As such, simple analysis of the terminal glycosylation status (Bjorklof et al., 2002) cannot be used as a surrogate marker for complete receptor maturation. The mutations introduced into TMD IV were clearly responsible for the reduction in 3-FRET signal observed in the TMD1 + TMD IV mutant. It is noteworthy that TMD IV has been implicated as a key 'dimer' interface in the D2 dopamine receptor (Guo et al., 2003; Lee et al., 2003) and, indeed, agonist and inverse agonist ligands alter the conformational details and structural organization of TMD IV of this receptor (Guo et al., 2005). The current studies demonstrate that the α_{1b} -adrenoceptor is able to organize into oligomers rather than simple dimers and that modification of the effectiveness of this process has major consequences for function. At this stage such studies have required levels of expression higher than generally reported for the α_{1b} -adrenoceptor in native tissues. The application of 3-FRET imaging with emerging generations of novel fluorescent proteins may allow assay sensitivity to be increased.

MOL #33035

REFERENCES

Baneres JL, and Parello J (2003) Structure-based analysis of GPCR function: evidence for a novel pentameric assembly between the dimeric leukotriene B4 receptor BLT1 and the G-protein. *J Mol Biol* **329**: 815-829.

Bernier V, Bichet DG and Bouvier M (2004) Pharmacological chaperone action on G-protein-coupled receptors. *Curr Opin Pharmacol* **4**: 528-533.

Bjorklof K, Lundstrom K, Abuin L, Greasley PJ and Cotecchia S (2002) Co- and posttranslational modification of the alpha(1B)-adrenergic receptor: effects on receptor expression and function. *Biochemistry* **41**: 4281-4291.

Bulenger S, Marullo S and Bouvier M (2005) Emerging role of homo- and heterodimerization in G-protein-coupled receptor biosynthesis and maturation. *Trends Pharmacol Sci* **26**: 131-137.

Carrillo JJ, López-Gimenez JF and Milligan G (2004) Multiple interactions between transmembrane helices generate the oligomeric α_{1b} -adrenoceptor. *Mol Pharmacol* **66**: 1123-1137.

Conn PM, Knollman PE, Brothers and Janovick JA (2006) Protein folding as post-translational regulation: evolution of a mechanism for controlled plasma membrane expression of a GPCR. *Mol Endocrinol* **20**: 3035-3041.

de Juan D, Mellado M, Rodriguez-Frade JM, Hernanz-Falcon P, Serrano A, Del Sol A, Valencia A, Martinez-A C and Rojas AM. (2005) A framework for computational and experimental methods: Identifying dimerization residues in CCR chemokine receptors. *Bioinformatics* **21 Suppl 2**:ii13-ii18.

MOL #33035

Ding WQ, Cheng ZJ, McElhiney J, Kuntz SM and Miller LJ (2002) Silencing of secretin receptor function by dimerization with a misspliced variant secretin receptor in ductal pancreatic adenocarcinoma. *Cancer Res* **62**: 5223-5229.

Duvernay MT, Filipeanu CM and Wu G (2005) The regulatory mechanisms of export trafficking of G protein-coupled receptors. *Cell Signal* **17**: 1457-1465.

Erickson MG, Moon DL and Yue DT (2003) DsRed as a potential FRET partner with CFP and GFP. *Biophys J* **85**: 599-611.

Fotiadis D, Liang Y, Filipek S, Saperstein DA, Engel A and Palczewski K (2004) The G protein-coupled receptor rhodopsin in the native membrane. *FEBS Lett* **564**: 281-288.

Franco R, Casado V, Mallol J, Ferrada C, Ferre S, Fuxe K, Cortes A, Ciruela F, Lluís C and Canela EI (2006) The two-state dimer receptor model: a general model for receptor dimers. *Mol Pharmacol* **69**: 1905-1912.

Galperin E, Verkhusha VV and Sorkin A (2004) Three-chromophore FRET microscopy to analyse multiprotein interactions in living cells. *Nature Methods* **1**: 209-217.

Guo W, Shi JA and Javitch JA (2003) The fourth transmembrane segment forms the interface of the dopamine D2 receptor homodimer. *J Biol Chem* **278**: 4385-4388.

Guo W, Shi L, Filizola M, Weinstein H and Javitch JA (2005) Crosstalk in G protein-coupled receptors: changes at the transmembrane homodimer interface determine activation. *Proc Natl Acad Sci U S A* **102**: 17495-17500.

MOL #33035

Herman B, Krishnan RV and Centonze VE (2004) Microscopic analysis of fluorescence resonance energy transfer (FRET). *Methods Mol Biol* **261**: 351-370.

Hernanz-Falcon P, Rodriguez-Frade JM, Serrano A, Juan D, del Sol A, Soriano SF, Roncal F, Gomez L, Valencia A, Martinez-A C, Mellado M. (2004). Identification of amino acid residues crucial for chemokine receptor dimerization. *Nat Immunol* **5**: 216-223.

Hu CD, Chinenov Y and Kerppola TK (2002) Visualization of interactions among bZIP and Rel family proteins in living cells using bimolecular fluorescence complementation. *Mol Cell* **9**: 789-798.

Kerppola TK (2006) Visualization of molecular interactions by fluorescence complementation. *Nat Rev Mol Cell Biol* **7**: 449-456.

Lee SP, O'Dowd BF, Rajaram RD, Nguyen T and George SR (2003) D2 dopamine receptor homodimerization is mediated by multiple sites of interaction, including an intermolecular interaction involving transmembrane domain 4. *Biochemistry* **42**: 11023-11031.

Liang Y, Fotiadis D, Filipek S, Saperstein DA, Palczewski K and Engel A (2003) Organization of the G protein-coupled receptors rhodopsin and opsin in native membranes. *J Biol Chem* **278**: 21655-21662.

Mansoor SE, Palczewski K and Farrens DL (2006) Rhodopsin self-associates in asolectin liposomes. *Proc Natl Acad Sci USA* **103**: 3060-3065.

Meyer BH, Segura J-M, Martinez KL, Hovius R, George N, Johnsson K and Vogel H (2006) FRET imaging reveals that functional neurokinin-1 receptors are

MOL #33035

monomeric and reside in membrane microdomains of live cells. *Proc Natl Acad Sci USA* **103**: 2138-2143.

Milligan G (2004) G protein-coupled receptor dimerization: function and ligand pharmacology. *Mol Pharmacol* **66**: 1-7.

Milligan G (2006) G-protein-coupled receptor heterodimers: pharmacology, function and relevance to drug discovery. *Drug Discovery Today* **11**: 541-549.

Milligan G and Bouvier M (2005) Methods to monitor the quaternary structure of G protein-coupled receptors. *FEBS J* **272**: 2914-2925.

Morris DP, Price RR, Smith MP, Lei B and Schwinn DA (2004) Cellular trafficking of human α_1 -adrenergic receptors is continuous and primarily agonist-independent. *Mol Pharmacol* **66**: 843-854.

Park PS and Wells JW (2004) Oligomeric potential of the M2 muscarinic cholinergic receptor. *J Neurochem* **90**: 537-548.

Park PS, Filipek S, Wells JW and Palczewski K (2004) Oligomerization of G protein-coupled receptors: past, present, and future. *Biochemistry* **43**: 15643-15656.

Pediani JD, Colston JF, Caldwell D, Milligan G, Daly CJ and McGrath JC (2005) β -arrestin dependent spontaneous α_{1a} -adrenoceptor endocytosis causes intracellular transportation of α -blockers via recycling compartments. *Mol Pharmacol* **67**: 992-1004.

Petaja-Repo UE, Hogue M, Laperriere A, Walker P and Bouvier M (2002) Export from the endoplasmic reticulum represents the limiting step in the maturation and cell surface expression of the human delta opioid receptor. *J Biol Chem* **275**: 13727-13736.

MOL #33035

Pfleger KD and Edine KA (2006) Illuminating insights into protein-protein interactions using bioluminescence resonance energy transfer (BRET).

Nat Methods **3**: 165-174.

Pietila EM, Tuusa JT, Apaja PM, Aatsinki JT, Hakalahti AE, Rajaniemi HJ and Petaja-Repo UE (2005) Inefficient maturation of the rat luteinizing hormone receptor. A putative way to regulate receptor numbers at the cell surface.

J Biol Chem **280**: 26622-26629.

Salahpour A, Angers S, Mercier JF, Lagace M, Marullo S and Bouvier M (2004) Homodimerization of the beta2-adrenergic receptor as a prerequisite for cell surface targeting. *J Biol Chem* **279**: 33390-33397.

Strange PG (2005) Oligomers of D2 dopamine receptors: evidence from ligand binding. *J Mol Neurosci* **26**: 155-160.

Ulloa-Aguirre A, Janovick JA, Brothers SP and Conn PM (2004) Pharmacologic rescue of conformationally-defective proteins: implications for the treatment of human disease. *Traffic* **5**: 821-837.

Wilson S, Wilkinson G and Milligan G (2005) The CXCR1 and CXCR2 receptors form constitutive homo- and heterodimers selectively and with equal apparent affinities. *J Biol Chem* **280**: 28663-28674.

MOL #33035

Footnotes

These studies were supported by the Medical Research Council and the Wellcome Trust.

MOL #33035

Figure Legends

Figure 1

Proposed oligomeric organization of the α_{1b} -adrenoceptor

Based on interactions between fragments of the α_{1b} -adrenoceptor, where TMD I and TMD IV (yellow) were shown to contribute symmetrical protein-protein interaction interfaces, Carrillo et al., (2004), proposed a 'daisy-chain' structure that may link α_{1b} -adrenoceptor monomers into higher-order oligomers. Cartoons of such oligomers are displayed: **Top**, viewed from the extracellular space, **Bottom** viewed as a section through the plasma membrane. Such organizational structure is reminiscent of the arrays of rhodopsin in murine rod outer segments observed by atomic force microscopy (Fotiadis et al., 2004).

Figure 2

Establishment of single cell 3 color FRET imaging using concatamers of fluorescent proteins

- A.** Concatamers of eCFP, eYFP and dsRed2 and eCFP, Tyr⁶⁷Cys eYFP with dsRed2, as well as a number of 2 protein open-reading frames were generated.
- B. (A₁-A₆).** The eCFP-eYFP-dsRed2 concatamer was expressed in HEK293 cells and imaged. Each element of the concatamer (**A₁**, eCFP, **A₂**, eYFP, **A₃**, dsRed2) could be monitored. Excitation at 430 nm allowed imaging of eCFP-eYFP (**A₄**) and eCFP-dsRed2 (**A₆**) FRET. Excitation at 495 nm allowed imaging of eYFP-dsRed2 (**A₅**) FRET. (**B₁-B₆**) The eCFP-Tyr⁶⁷Cys eYFP-dsRed2 concatamer was expressed in HEK293 cells and imaged. Although

MOL #33035

the eCFP (**B**₁) and dsRed2 (**B**₃) elements could be visualized, Tyr⁶⁷Cys eYFP is not fluorescent (**B**₂). **B**₄-**B**₆. FRET signals akin to **A**₄-**A**₆ are shown. (**C**₁-**C**₆) Individual forms of **C**₁, eCFP, **C**₂, eYFP, **C**₃, dsRed2 were co-expressed **C**₄-**C**₆. FRET signals were monitored. Pseudo-color images of FRET signals are coded according to the normalized FRET calculations (see Materials and Methods and Supplementary data). **C**. The basis of direct eCFP-dsRed2 and sequential eCFP-eYFP-dsRed2 FRET is illustrated. **D**. Various 2 protein open-reading frames and the 3 protein concatamers were expressed or the individual fluorescent proteins co-expressed. FRET signals were quantitated and normalized (see Materials and Methods and Supplementary data). These were used to establish appropriate conditions to measure both direct 2 protein eCFP-dsRed2 and sequential 3 protein eCFP-eYFP-dsRed2 FRET. 1.0 is equivalent to no FRET signal.

Figure 3

Single cell imaging of oligomers of the α_{1b} -adrenoceptor containing at least 3 monomers. Combined mutations in TMD I and TMD IV modify oligomeric organization

A. Forms of the α_{1b} -adrenoceptor N-terminally tagged (**black**) with the FLAG epitope were C-terminally tagged with eCFP, eYFP or dsRed2 whilst an N-terminally c-myc tagged form of the α_{1b} -adrenoceptor was C-terminally tagged with Tyr⁶⁷Cys eYFP. FLAG-tagged forms of Leu⁶⁵Ala, Val⁶⁶Ala, Leu¹⁶⁶Ala, Leu¹⁶⁷Ala α_{1b} -adrenoceptor were C-terminally tagged with either

MOL #33035

eCFP or eYFP and a c-myc tagged form of Leu⁶⁵Ala, Val⁶⁶Ala, Leu¹⁶⁶Ala, Leu¹⁶⁷Ala α_{1b} -adrenoceptor with dsRed2. **X** indicates sites of mutation.

B. (A₁-A₆) FLAG-tagged forms of α_{1b} -adrenoceptor-eCFP (**A₁**), α_{1b} -adrenoceptor-eYFP (**A₂**) and α_{1b} -adrenoceptor-dsRed2 (**A₃**) were co-expressed in HEK293 cells. (**B₁-B₆**). Equivalent forms of Leu⁶⁵Ala, Val⁶⁶Ala, Leu¹⁶⁶Ala, Leu¹⁶⁷Ala α_{1b} -adrenoceptor were expressed and imaged, **B₁**; eCFP, **B₂**, eYFP, **B₃**, dsRed2. FRET signals following excitation as in Figure 2 were imaged (**A₄-A₆**, **B₄-B₆**). **C.** eCFP-dsRed2 FRET signals were normalized for the wild type α_{1b} -adrenoceptor (**black**), α_{1b} -adrenoceptor with Tyr⁶⁷CysYFP as one of the constructs (**gray**) and Leu⁶⁵Ala, Val⁶⁶Ala, Leu¹⁶⁶Ala, Leu¹⁶⁷Ala α_{1b} -adrenoceptor (**white**). Sequential 3 protein FRET was calculated by subtracting the signal in cells expressing α_{1b} -adrenoceptor-Tyr⁶⁷CysYFP. * Significantly lower ($p < 0.05$).

D. α_{1b} -adrenoceptor-Tyr⁶⁷Cys eYFP is non-fluorescent but is expressed. α_{1b} -adrenoceptor-eCFP (**A₁,B₁**) and α_{1b} -adrenoceptor-dsRed2 (**A₃,B₃**) were co-expressed with c-myc- α_{1b} -adrenoceptor-Tyr⁶⁷Cys eYFP (**A₂,B₂**). (**A₁-A₃**) fluorescence imaging, (**B₁-B₃**) cells were permeabilized and immunoblotted with anti-c-myc and secondary antibody and either direct fluorescence (**B₁, B₃**) or immunofluorescence (**B₂**) images obtained.

Figure 4

The wild type α_{1b} -adrenoceptor but not Leu⁶⁵Ala, Val⁶⁶Ala, Leu¹⁶⁶Ala, Leu¹⁶⁷Ala α_{1b} -adrenoceptor is able to reach the cell surface

MOL #33035

A. HEK293 cells were transfected to express FLAG-tagged forms of wild type α_{1b} -adrenoceptor-eYFP (**A, B**) or Leu⁶⁵Ala, Val⁶⁶Ala, Leu¹⁶⁶Ala,Leu¹⁶⁷Ala α_{1b} -adrenoceptor-eYFP (**C, D**). Non-permeabilized (**A, C**) and permeabilized (**B, D**) cells were stained with anti-FLAG and secondary antibody and imaged to detect eYFP (**A₁, B₁, C₁, D₁**) or anti-FLAG (**A₂, B₂, C₂, D₂**). eYFP and anti-FLAG images were also merged (**A₃, B₃, C₃, D₃**). **B.** Cells expressing wild type α_{1b} -adrenoceptor-eYFP (**A₁-A₄**) or Leu⁶⁵Ala, Val⁶⁶Ala, Leu¹⁶⁶Ala,Leu¹⁶⁷Ala α_{1b} -adrenoceptor-YFP (**B₁-B₄**) were treated with Hoechst 33342 nuclear stain and RQAPB for 30 min and imaged; **A₁,B₁** YFP; **A₂,B₂** Hoechst 33342; **A₃,B₃** RQAPB; **A₄,B₄** merged images.

Figure 5

The Leu⁶⁵Ala, Val⁶⁶Ala, Leu¹⁶⁶Ala,Leu¹⁶⁷Ala α_{1b} -adrenoceptor is not terminally glycosylated

A. Membranes from mock transfected HEK293 cells (**open circles**) and those transfected to express FLAG- α_{1b} -adrenoceptor-eYFP (**filled squares**) or FLAG Leu⁶⁵Ala, Val⁶⁶Ala, Leu¹⁶⁶Ala,Leu¹⁶⁷Ala α_{1b} -adrenoceptor-eYFP (**open squares**) were used to monitor fluorescence corresponding to eYFP.

B. The specific binding of varying concentrations of [³H]prazosin to FLAG- α_{1b} -adrenoceptor-eYFP (**upper panel**) and FLAG-Leu⁶⁵Ala, Val⁶⁶Ala, Leu¹⁶⁶Ala,Leu¹⁶⁷Ala α_{1b} -adrenoceptor-eYFP (**lower panel**) was assessed.

C. Membranes expressing α_{1b} -adrenoceptor-eYFP (**1**) or Leu⁶⁵Ala, Val⁶⁶Ala, Leu¹⁶⁶Ala,Leu¹⁶⁷Ala α_{1b} -adrenoceptor-eYFP (**2**) were resolved by SDS-PAGE and immunoblotted with anti-GFP.

MOL #33035

D. For α_{1b} -adrenoceptor-eYFP the band of apparent Mr 75 kDa is the immature form of the receptor and the band of apparent Mr 105 kDa the mature, terminally N-glycosylated form. Membranes expressing wild type α_{1b} -adrenoceptor-eYFP were treated with vehicle (**1**) or N-glycosidase F (**2**), and then resolved and immunoblotted as in **C**.

Figure 6

Monitoring α_{1b} -adrenoceptor quaternary structure via bi-molecular fluorescence complementation

N-terminally FLAG-tagged forms of the α_{1b} -adrenoceptor were C-terminally tagged with either the N-terminal 172 amino acids (**A**, **C**) or C-terminal 67 amino acids (**B**, **C**) of eYFP. Cells were either imaged to detect bi-molecular fluorescence complementation (**upper row**) or permeabilized cells were used to detect the FLAG epitope (**lower row**).

Figure 7

Bi-molecular fluorescence complementation and RQAPB labelling demonstrates the α_{1b} -adrenoceptor is recycling in cells as a dimer/oligomer and Leu⁶⁵Ala, Val⁶⁶Ala, Leu¹⁶⁶Ala, Leu¹⁶⁷Ala α_{1b} -adrenoceptor retains quaternary structure but is retained in the endoplasmic reticulum

N-terminally FLAG-tagged forms of the α_{1b} -adrenoceptor were C-terminally tagged with the N-terminal 172 or C-terminal 67 amino acids of eYFP and expressed in HEK293 cells (**A**). RQAPB was subsequently added. Cell nuclei (**A₁**) were stained

MOL #33035

with Hoechst 33342 nuclear dye, bi-molecular fluorescence complementation (**A**₂) was assessed via eYFP fluorescence, whilst previous cell surface delivery of the α_{1b} -adrenoceptor was shown by the appearance (**A**₃) of red fluorescence corresponding to ligand binding. Merging of the images (**A**₄) produced a strong overlap correlation coefficient for the receptor dimer/oligomer and bound RQAPB ($r^2=0.84$).

c-myc-Leu⁶⁵Ala, Val⁶⁶Ala, Leu¹⁶⁶Ala,Leu¹⁶⁷Ala α_{1b} -adrenoceptor was C-terminally tagged with the N-terminal 172 amino acids of eYFP whilst FLAG- Leu⁶⁵Ala, Val⁶⁶Ala, Leu¹⁶⁶Ala,Leu¹⁶⁷Ala α_{1b} -adrenoceptor was C-terminally tagged with the C-terminal 67 amino acids of eYFP (**B**). Following transfection into HEK293 cells RQAPB was added. Cell nuclei (**B**₁) were stained with Hoechst 33342 nuclear dye, bi-molecular fluorescence complementation (**B**₂) was assessed via eYFP fluorescence, whilst lack of cell surface delivery of Leu⁶⁵Ala, Val⁶⁶Ala, Leu¹⁶⁶Ala,Leu¹⁶⁷Ala α_{1b} -adrenoceptor was shown by the lack of development (**B**₃) of Red fluorescence corresponding to ligand binding. The merged image (**B**₄) confirms the perinuclear location of the Leu⁶⁵Ala, Val⁶⁶Ala, Leu¹⁶⁶Ala,Leu¹⁶⁷Ala α_{1b} -adrenoceptor dimer/oligomer.

Figure 8

Cells expressing the wild type but not Leu⁶⁵Ala, Val⁶⁶Ala, Leu¹⁶⁶Ala,Leu¹⁶⁷Ala α_{1b} -adrenoceptor respond to phenylephrine

Cells transfected to express wild type α_{1b} -adrenoceptor-eYFP (**A, C green**), or

MOL #33035

Leu⁶⁵Ala, Val⁶⁶Ala, Leu¹⁶⁶Ala, Leu¹⁶⁷Ala α_{1b} -adrenoceptor-eCFP (**A, C red**,) were loaded with Fura-2 and stimulated sequentially with 10 μ M phenylephrine (**B, C**) and ATP (**C**). In **A** the group of cells on the left of the image (red) express Leu⁶⁵Ala, Val⁶⁶Ala, Leu¹⁶⁶Ala, Leu¹⁶⁷Ala α_{1b} -adrenoceptor-eCFP and the group on the right (green) express wild type α_{1b} -adrenoceptor-eYFP. **B**. Peak Ca²⁺ signals following addition of phenylephrine. Only cells expressing α_{1b} -adrenoceptor-eYFP respond to phenylephrine (arrow). Picture taken 30 sec after addition of phenylephrine.

Figure 9

Ligand binding characteristics of the wild type and Leu⁶⁵Ala, Val⁶⁶Ala, Leu¹⁶⁶Ala, Leu¹⁶⁷Ala α_{1b} -adrenoceptor

The capacity of phenylephrine to compete for binding with [³H] prazosin to the wild type (filled symbols) and Leu⁶⁵Ala, Val⁶⁶Ala, Leu¹⁶⁶Ala, Leu¹⁶⁷Ala (open symbols) α_{1b} -adrenoceptor-eYFP was assessed. The graph corresponds to a representative result from three independent experiments. Wild type α_{1b} -adrenoceptor-eYFP ($pK_i = 4.82 \pm 0.25$), Leu⁶⁵Ala, Val⁶⁶Ala, Leu¹⁶⁶Ala, Leu¹⁶⁷Ala α_{1b} -adrenoceptor-eYFP (pK_i *high* = 8.41 ± 0.16 ; pK_i *low* = 6.35 ± 0.14 ; % *high* = 26.10 ± 4.40).

Figure 10

Functional cell surface α_{1b} -adrenoceptors can be measured at vanishingly low levels

MOL #33035

Cells transfected to express wild type α_{1b} -adrenoceptor-eYFP (**A, C green**), or HEK293 cells were transiently transfected with varying amounts of cDNA encoding FLAG- α_{1b} -adrenoceptor-eYFP.

A. Membranes of these cells were used to measure the specific binding of a single concentration (0.4 nM) of [3 H]prazosin anticipated to bind more than 90% of the available sites (see Figure 5).

B. Varying amounts of these membranes were used to monitor fluorescence corresponding to eYFP.

C. Cells mock transfected (purple) or transfected with varying amounts (see Figure) of cDNA encoding FLAG- α_{1b} -adrenoceptor-eYFP were loaded with Fura-2 and monitored for intracellular Ca^{2+} signals following stimulation with 10 μ M phenylephrine and subsequently with 10 μ M ATP (only in mock transfected cells).

Figure 11

Co-expression with Leu⁶⁵Ala, Val⁶⁶Ala, Leu¹⁶⁶AlaLeu¹⁶⁷Ala α_{1b} -adrenoceptor limits cell surface delivery of the wild type α_{1b} -adrenoceptor but not the CXCR1 receptor

HEK293 cells were transfected to express either c-myc- α_{1b} -adrenoceptor Y⁶⁷C eYFP alone (**A**) or together with FLAG-Leu⁶⁵Ala, Val⁶⁶Ala, Leu¹⁶⁶AlaLeu¹⁶⁷Ala α_{1b} -adrenoceptor-eYFP in a 1:3 ratio (**B, C**). Immunocytochemistry was performed in non-permeabilized (**A, B**) or permeabilized (**C**) cells using an anti-c-myc antibody and a secondary antibody conjugated to Alexa594 (**red**) whilst monitoring eYFP (**green**) provided a measure of FLAG-Leu⁶⁵Ala, Val⁶⁶Ala, Leu¹⁶⁶Ala, Leu¹⁶⁷Ala α_{1b} -

MOL #33035

adrenoceptor expression and distribution. Nuclei were identified with Hoechst 33342 nuclear dye (**blue**). Merging of the images showed clear intracellular co-localization of the two forms of the receptor following their co-expression (**C**). Cells were co-transfected with FLAG-Leu⁶⁵Ala,Val⁶⁶Ala, Leu¹⁶⁶AlaLeu¹⁶⁷Ala α_{1b} -adrenoceptor-eYFP and c-myc-CXCR1 (**D**). Cell surface anti-c-myc staining (**red**), corresponding to the CXCR1 receptor, was observed in non-permeabilized cells expressing both high and low levels of eYFP fluorescence (**green**).

Figure 12

Mutations in TMD IV but not TMD I reduce 3-FRET signals

3-FRET studies were performed as in Figures 1 and 2 using HEK293 cells transfected to express each of eCFP, eYFP and dsRed2 tagged forms of wild type- (WT), Leu⁶⁵Ala, Val⁶⁶Ala (TM I), Leu¹⁶⁶Ala,Leu¹⁶⁷Ala (TM IV), and Leu⁶⁵Ala,Val⁶⁶Ala, Leu¹⁶⁶Ala, Leu¹⁶⁷Ala (TMI TMIV) α_{1b} -adrenoceptor. Data are means +/- S.E.M. n = 3, * significantly lower (p < 0.05) than wild type.

Figure 13

Although both TMD I and TMD IV mutants of the α_{1b} -adrenoceptor mature to be terminally N-glycosylated neither is delivered to the plasma membrane

A. HEK293 cells were transfected to express FLAG-tagged forms of wild type α_{1b} -adrenoceptor-eYFP (**A**), Leu⁶⁵Ala,Val⁶⁶Ala α_{1b} -adrenoceptor-eYFP (**B**), or Leu¹⁶⁶Ala,Leu¹⁶⁷Ala α_{1b} -adrenoceptor-eYFP (**C**). Non-permeabilized cells were

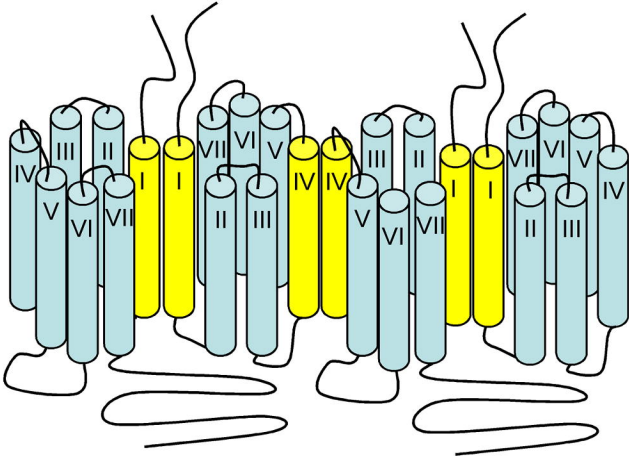
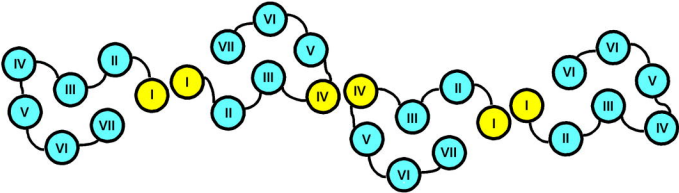
MOL #33035

stained with anti-FLAG and secondary antibody and imaged to detect eYFP (**A₁, B₁, C₁**) or anti-FLAG (**A₂, B₂, C₂**).

B. Cells expressing Leu⁶⁵Ala, Val⁶⁶Ala α_{1b} -adrenoceptor-eYFP (**A₁-A₄**) or Leu¹⁶⁶Ala,Leu¹⁶⁷Ala α_{1b} -adrenoceptor-eYFP (**B₁-B₄**) were treated with Hoechst 33342 nuclear stain and RQAPB for 30 min and imaged; **A₁,B₁** Hoechst 33342; **A₂,B₂** YFP; **A₃,B₃** RQAPB; **A₄,B₄** merged images.

C. Membranes expressing α_{1b} -adrenoceptor-eYFP (**1**), Leu⁶⁵Ala, Val⁶⁶Ala, Leu¹⁶⁶Ala,Leu¹⁶⁷Ala α_{1b} -adrenoceptor-eYFP (**2**), Leu⁶⁵Ala, Val⁶⁶Ala α_{1b} -adrenoceptor-eYFP (**3**) or Leu¹⁶⁶Ala,Leu¹⁶⁷Ala α_{1b} -adrenoceptor-eYFP (**4**) were resolved by SDS-PAGE and immunoblotted with anti-FLAG.

Figure 1



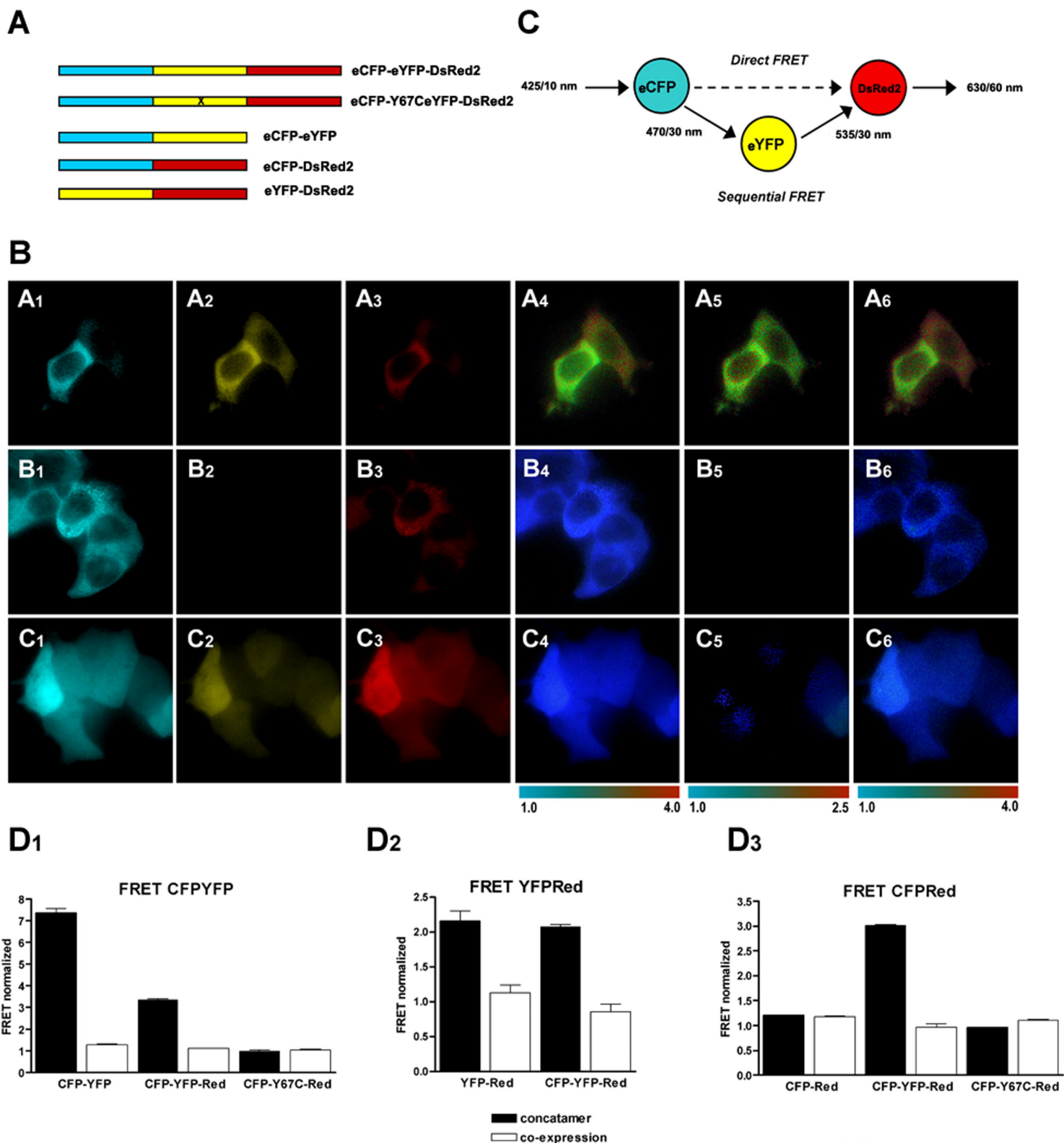
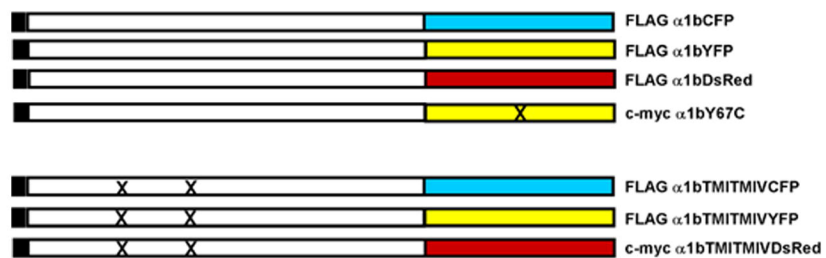
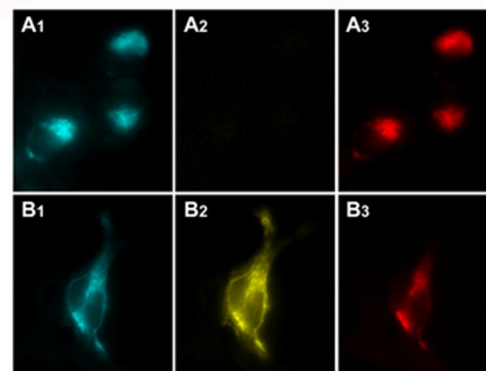
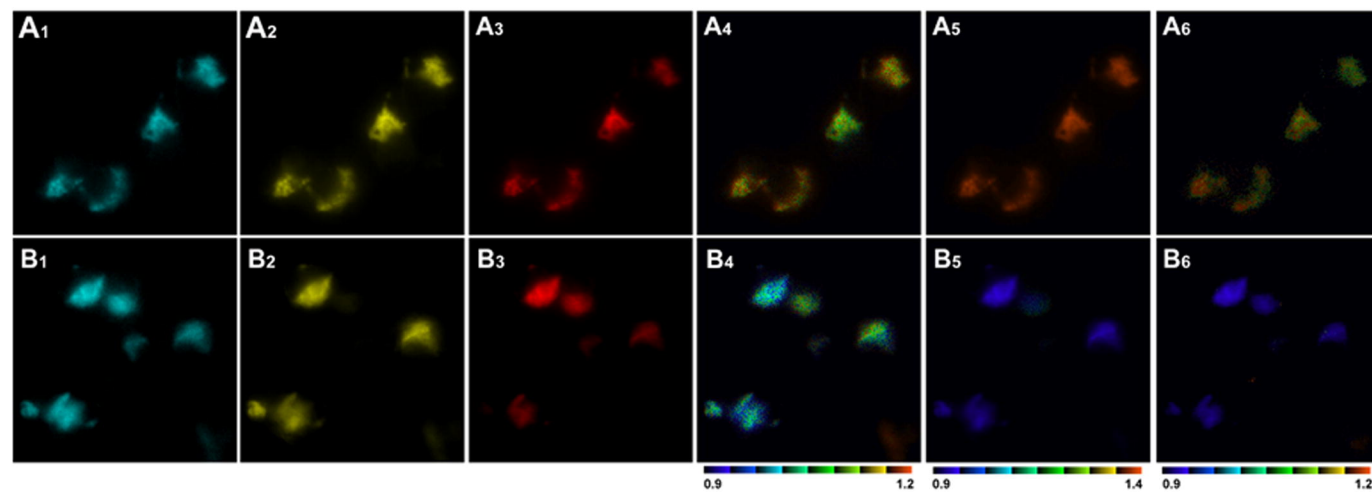
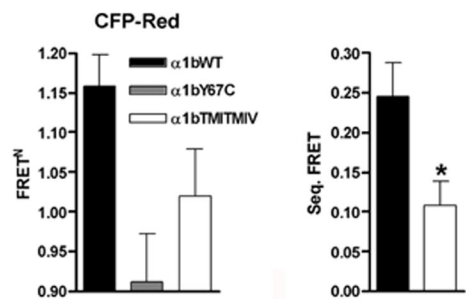
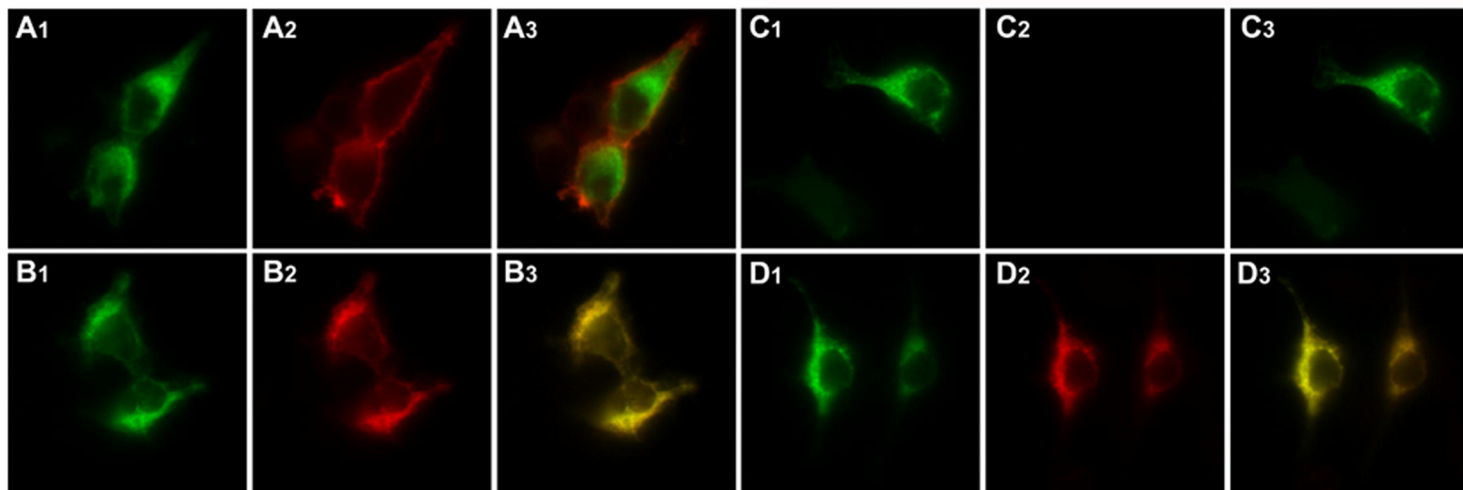
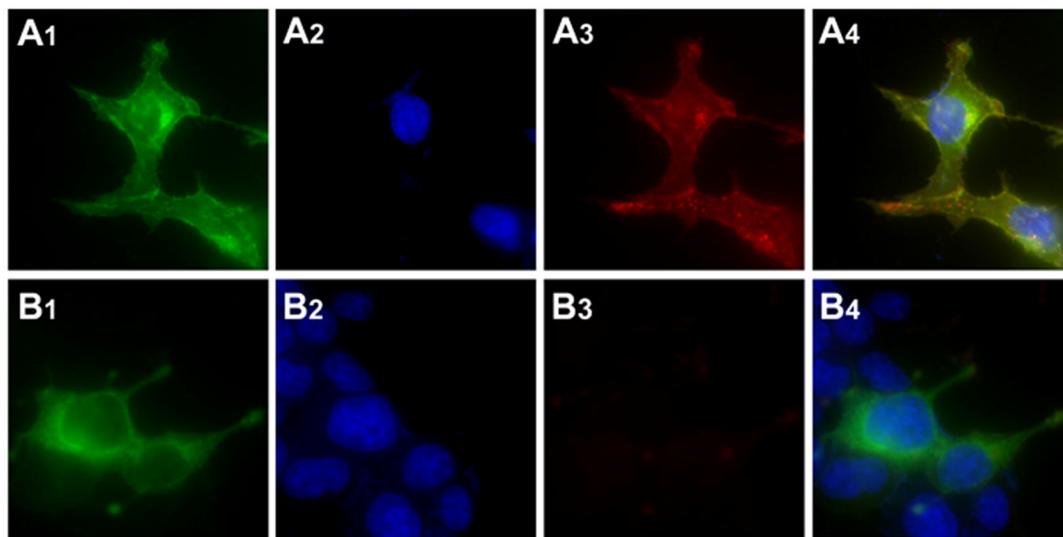
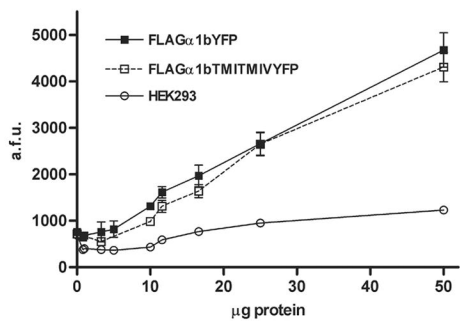
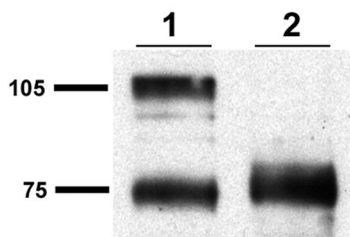
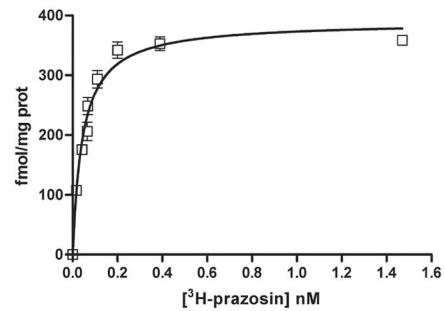
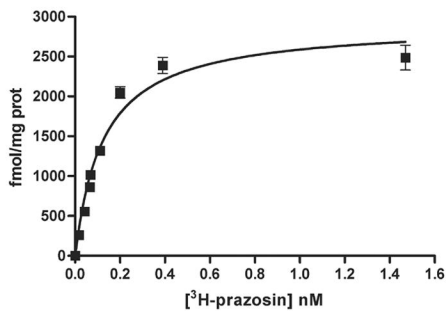
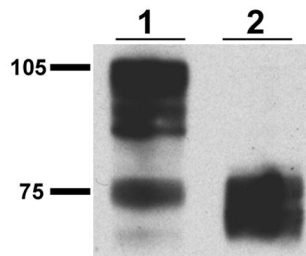


Figure 2

A**D****B****C****Figure 3**

A**B****Figure 4**

A**C****B****D****Figure 5**

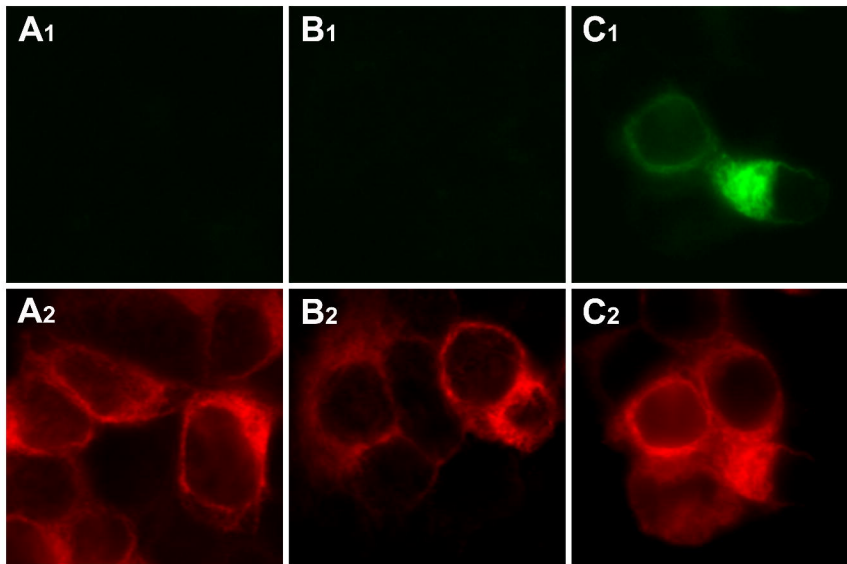


Figure 6

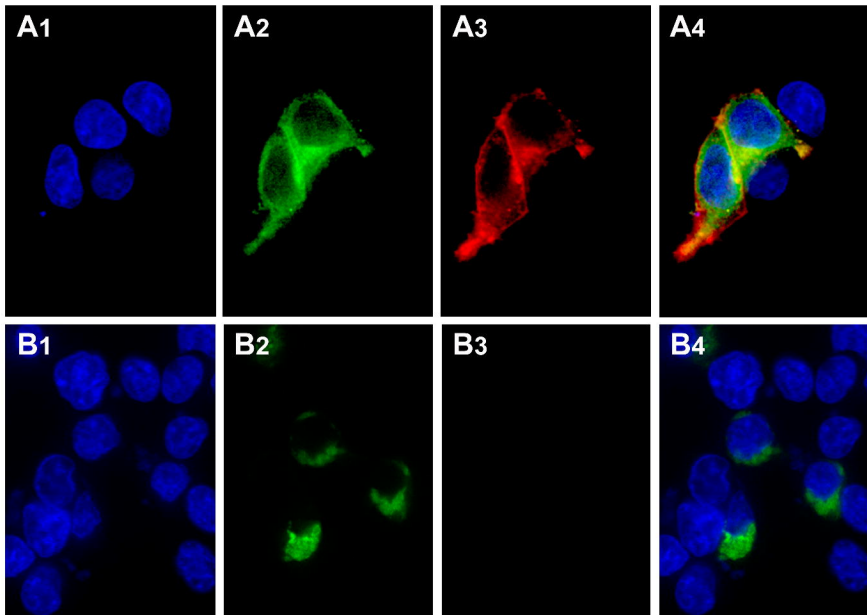


Figure 7

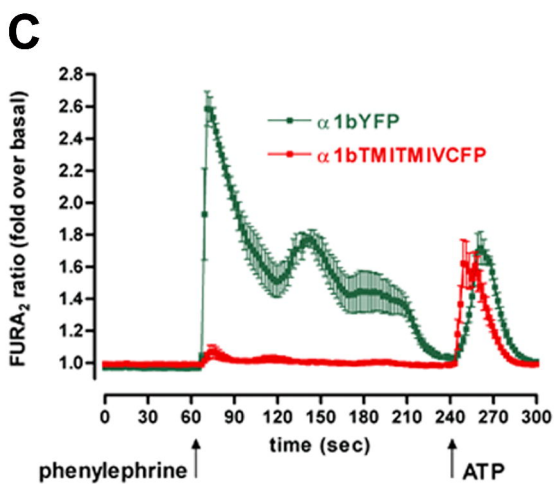
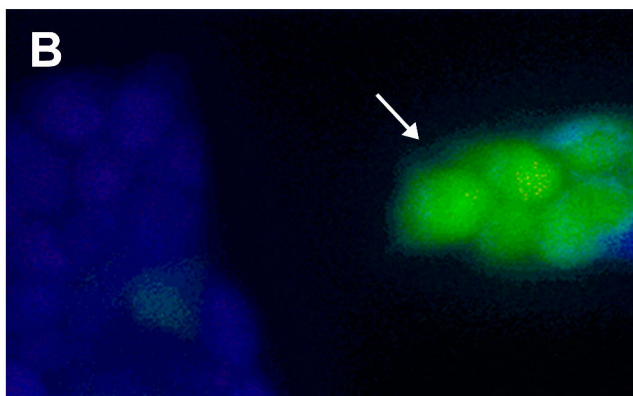
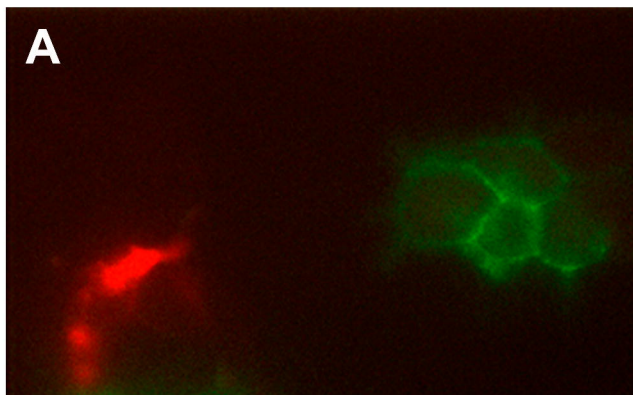


Figure 8

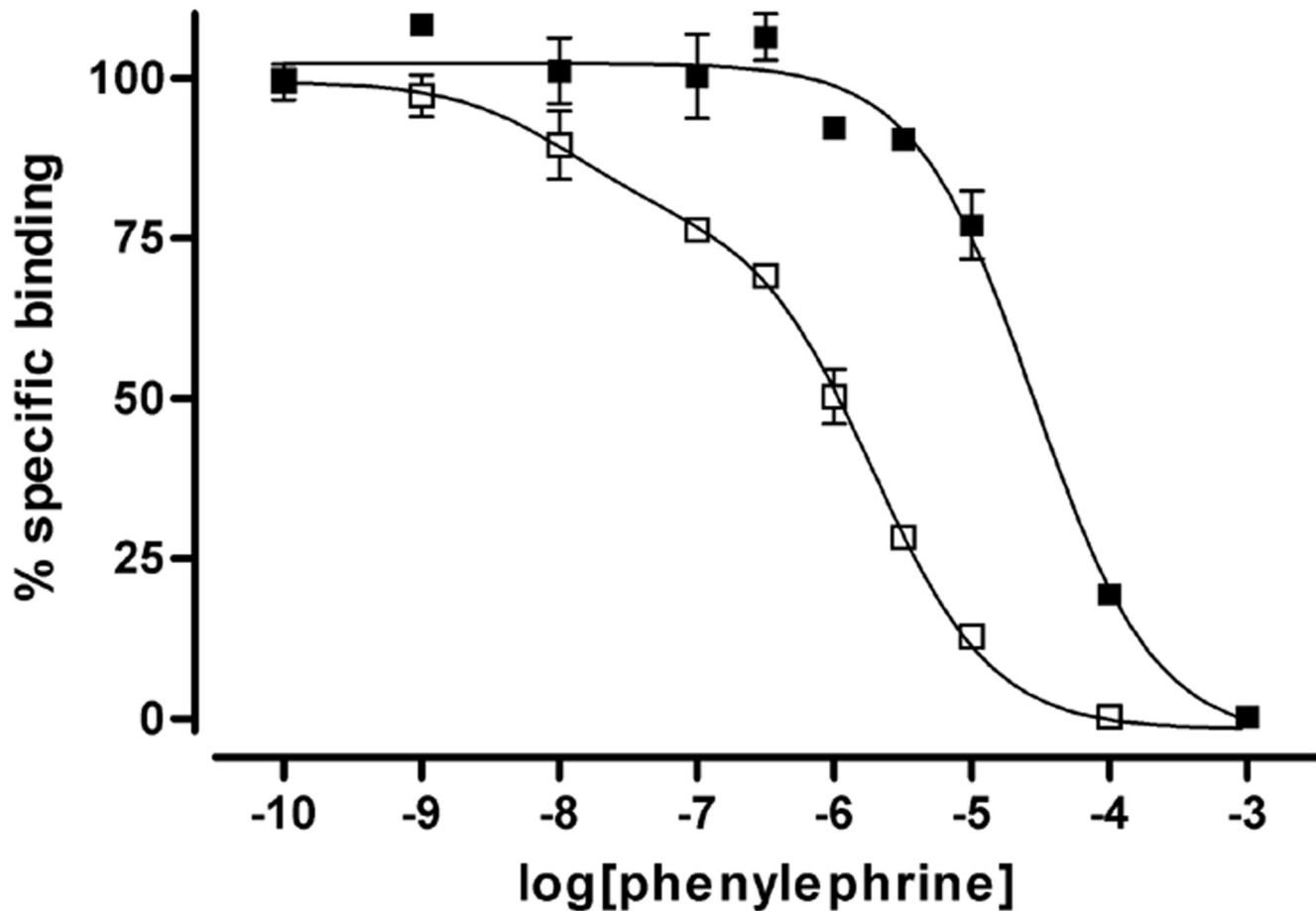
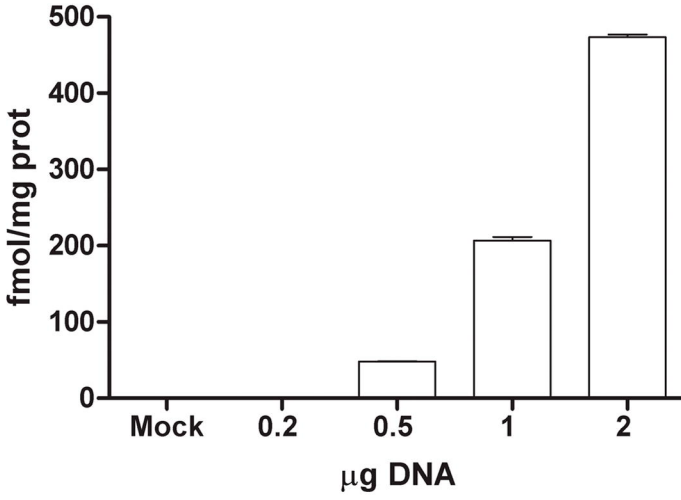
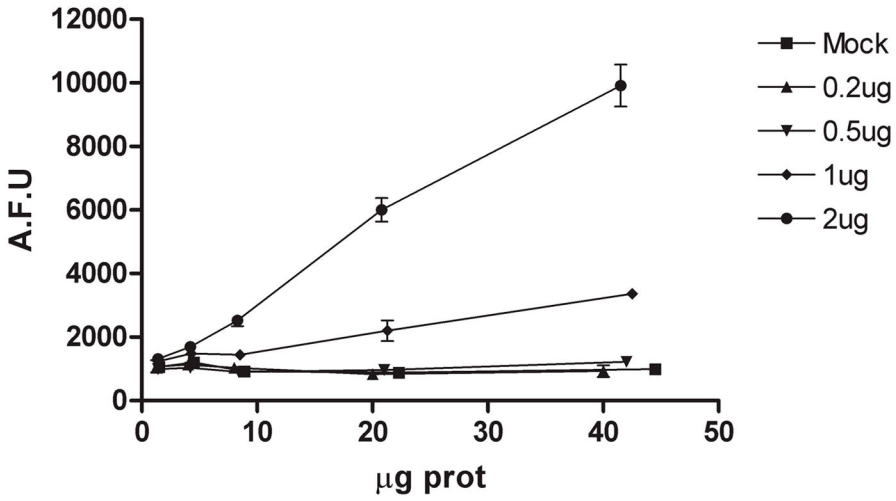


Figure 9

A



B



C

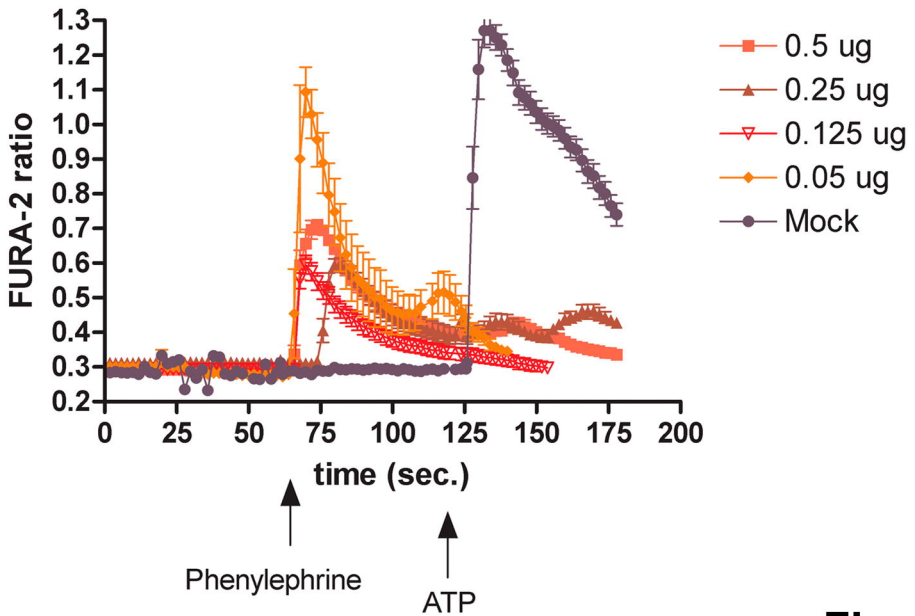


Figure 10

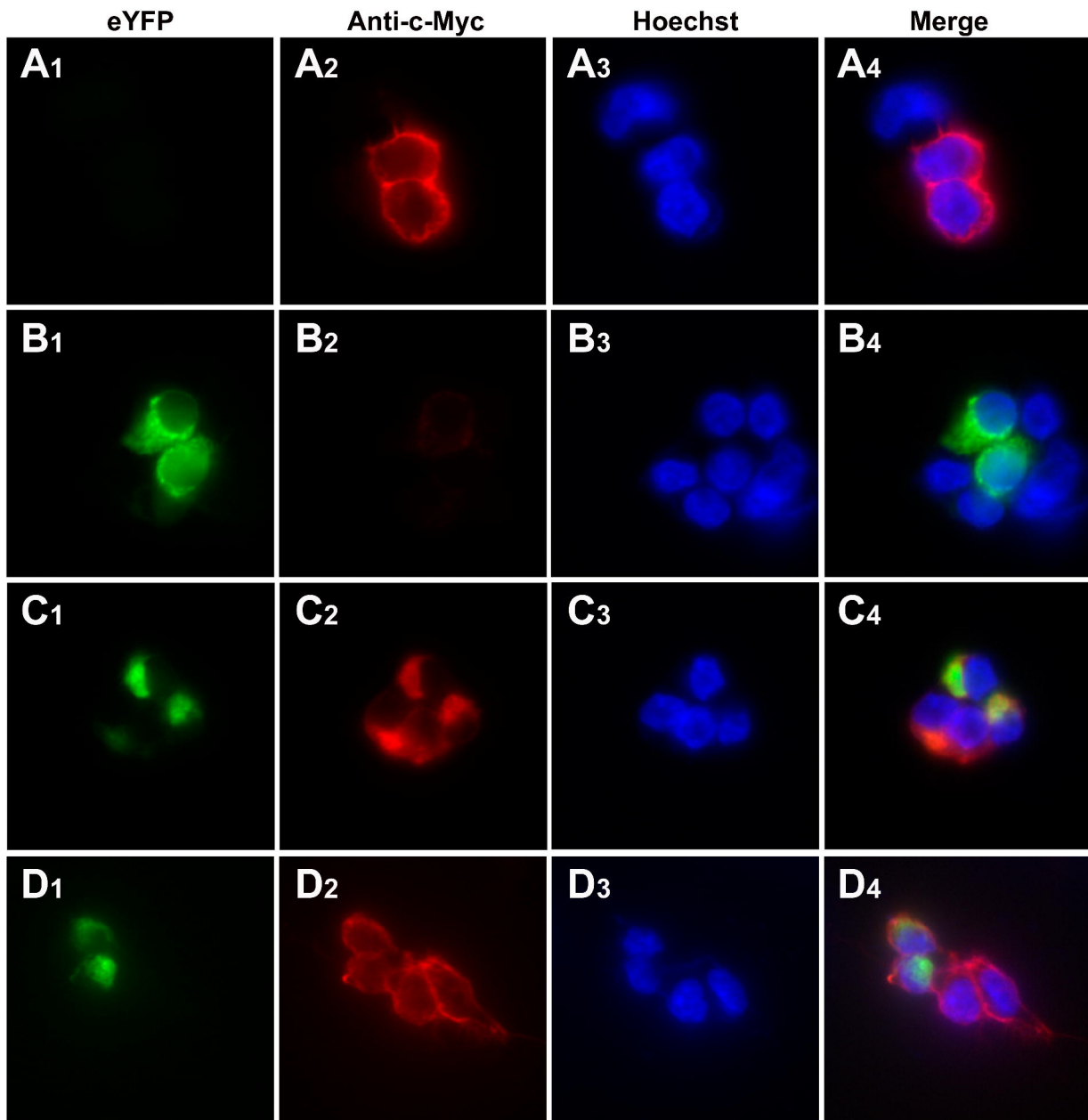


Figure 11

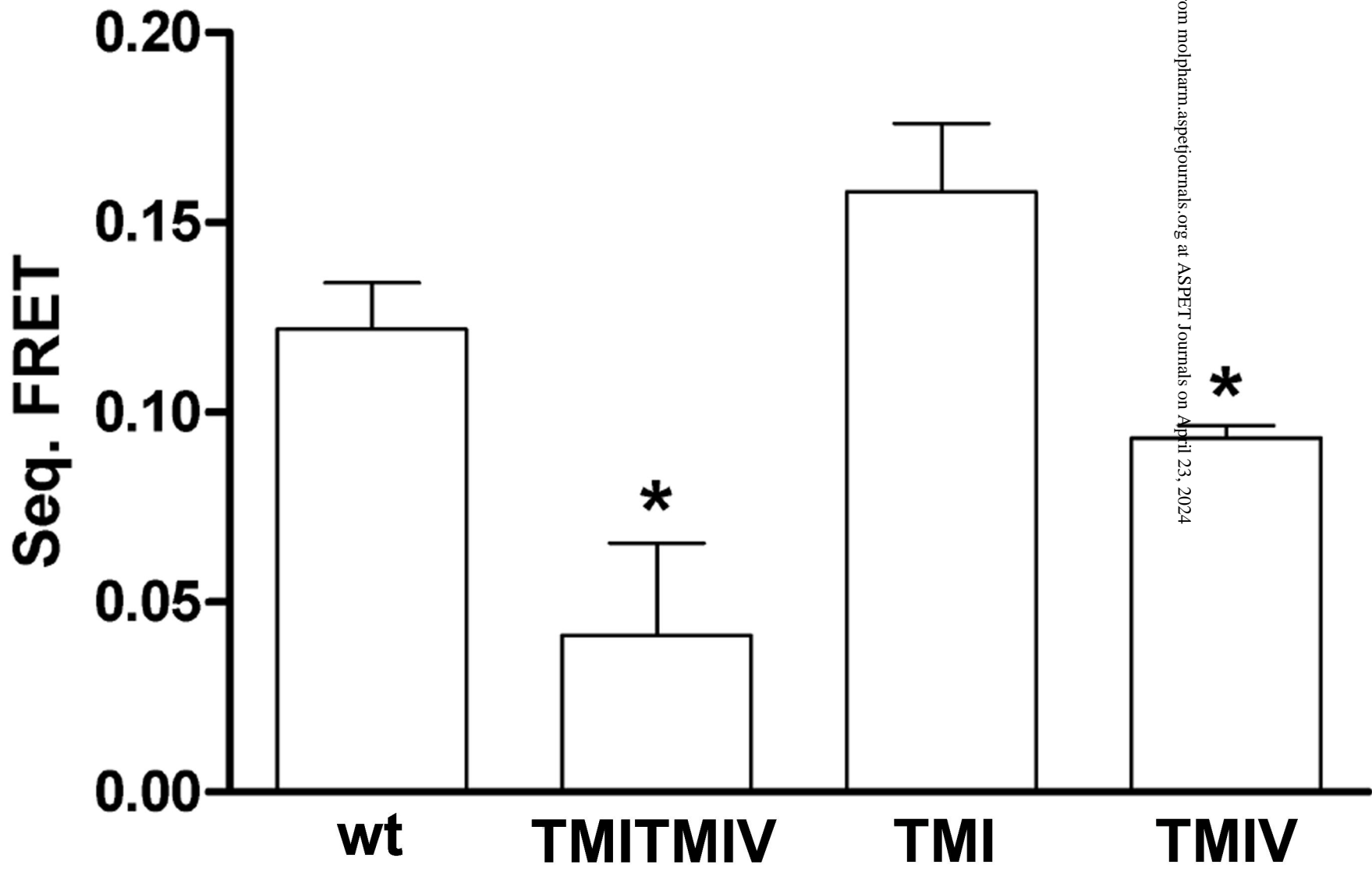
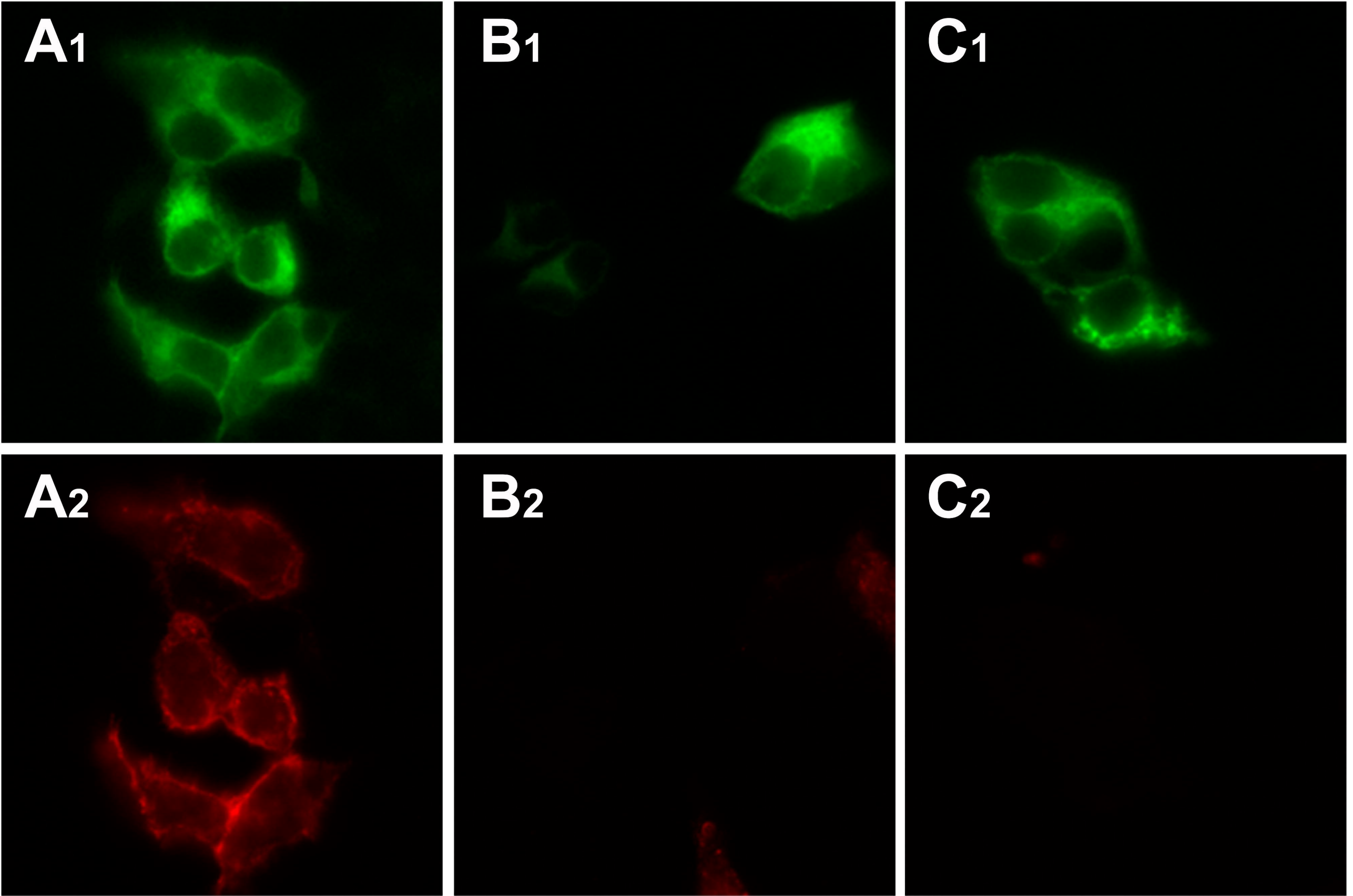
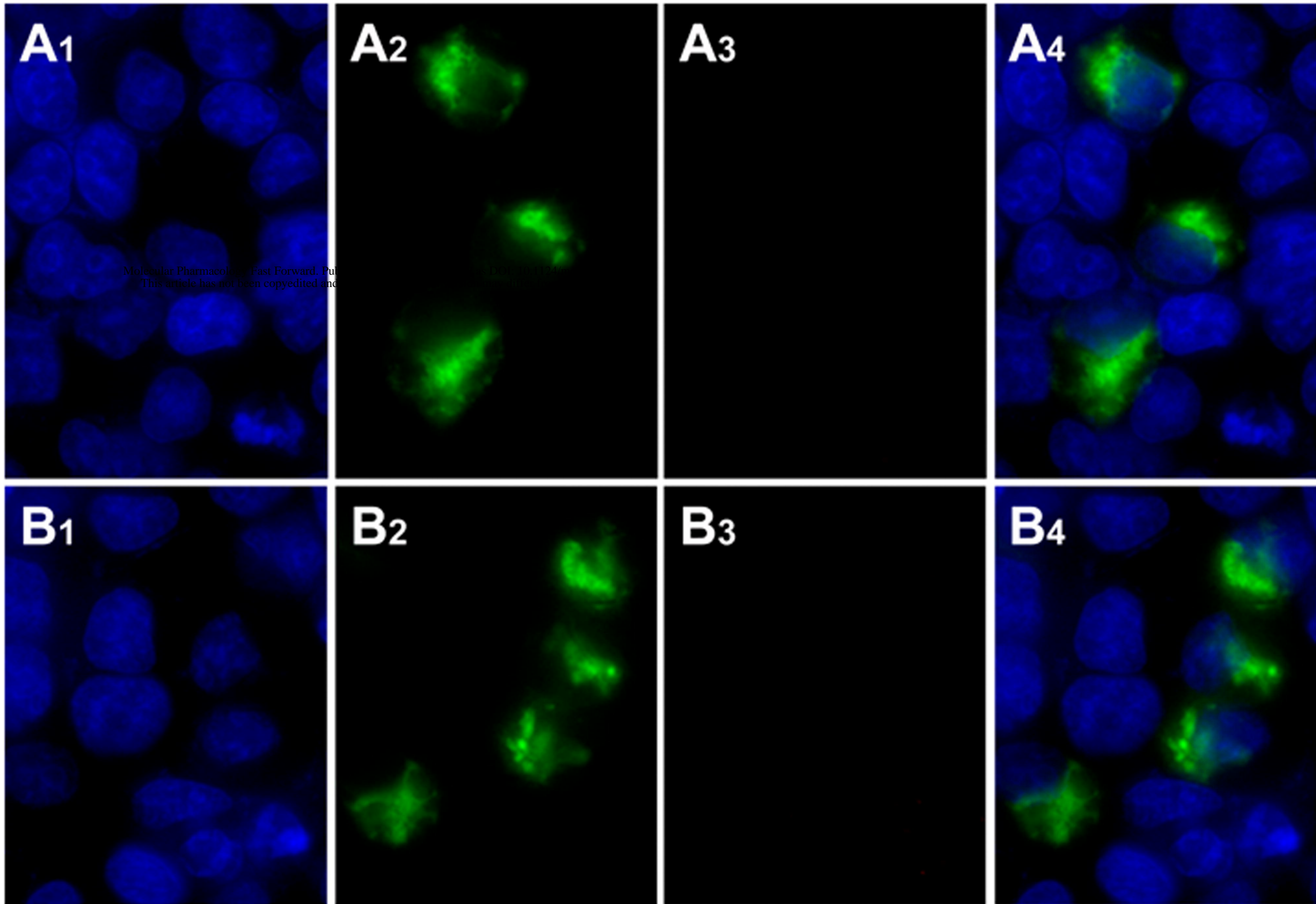
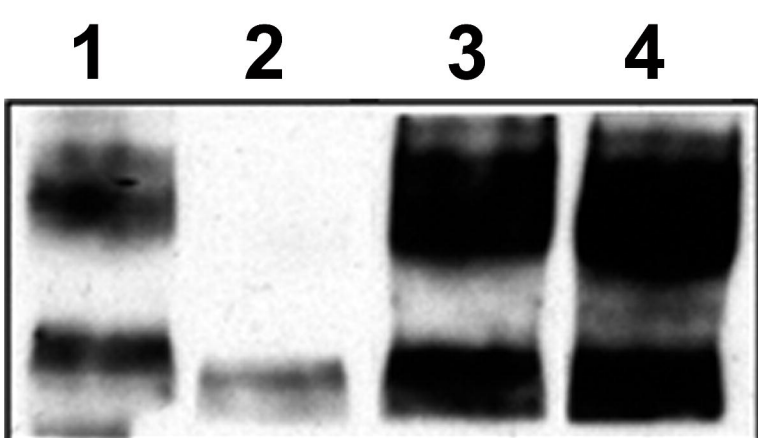


Figure 12

A**B****C**

Molecular Pharmacology: Fast Forward, Pub
 This article has not been certified by
 on April 23, 2024

Figure 13